AD-A118 641 PRINCETON UNIV NJ DEPT OF MECHANICAL AND AEROSPACE --ETC F/G 21/2
HIGH TEMPERATURE CATALYTICALLY ASSISTED COMBUSTION.(U)
AUG 81 C BRUNO, F V BRACCO, B S ROYCE AFOSR-76-3052
UNCLASSIFIED AFOSR-TR-82-0666 NL

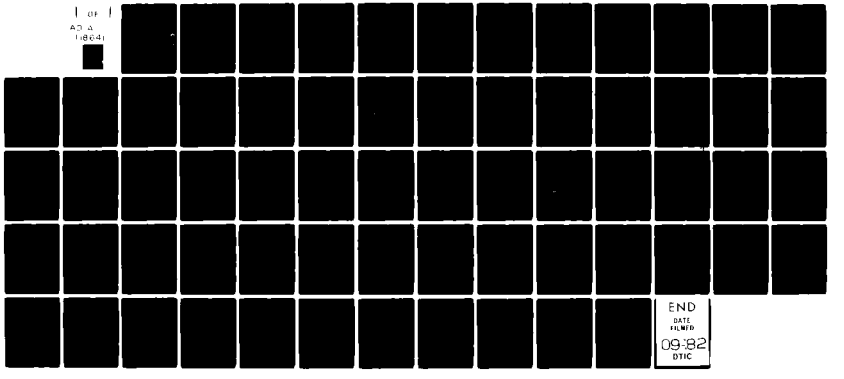

(4)

High Temperature Catalytically Assisted Combustion

Final

AFOSR-76-3052

STATEMENT OF WORK

AF FUNCTION - Weapon delivery and defenses, transport, advanced air-breathing engines.

DEFICIENCY - Insufficient understanding of the basic physical, chemical and fluid dynamic processes of ignition, stability, and efficiency of catalytic combustion. Lack of guidelines for predicting catalytic combustor performance and for solution of existing combustor difficulties.

OBJECTIVE - To clarify the relative importance, and to formulate realistic analytical representation of homogeneous, heterogeneous kinetics and transport processes in catalytic combustion phenomena associated with advanced air-breathing combustion systems.

HOW WORK CONTRIBUTES - Will provide additional understanding and needed realistic analytical modeling of homogeneous and heterogeneous high temperature catalytic combustion processes not now available. Will contribute to establishing realistic guidelines and techniques for the design of efficient, stable, jet engine catalytic combustors.

APPROACH - Theoretical and experimental studies will be made of basic fluid dynamic, physical and chemical processes in catalytic combustion associated with air-breathing propulsion systems. The relative importance of gas phase kinetics, heat transfer, mass diffusion, and surface chemical kinetics will be assessed. The practical phenomena will be experimentally simulated. Deficiencies in existing mathematical models will be demonstrated and improved models formulated based on experimental data and field observations. Various monolithic and packed-bed catalyst candidates for advanced combustor design will be studied over a range of operating conditions characteristic of advanced air-breathing propulsion engines with various hydrocarbon fuels. The two-dimensional model for laminar and turbulent boundary layers with multiple gas and surface reactions

UNCLASSIFIED

SECURITY CLASSIFICATION OF THIS PAGE (When Data Entered)

REPORT DOCUMENTATION PAGE		READ INSTRUCTIONS BEFORE COMPLETING FORM
1. REPORT NUMBER AFOSR-TR- 82-0666	2. GOVT ACCESSION NO. AD A118641	3. RECIPIENT'S CATALOG NUMBER
4. TITLE (and Subtitle) HIGH TEMPERATURE CATALYTICALLY ASSISTED COMBUSTION		5. TYPE OF REPORT & PERIOD COVERED FINAL 1 June 80 - 31 May 81 6. PERFORMING ORG. REPORT NUMBER
7. AUTHOR(s) C BRUNO P M CURTIS F V BRACCO B S H ROYCE		8. CONTRACT OR GRANT NUMBER(s) AFOSR-76-3052
9. PERFORMING ORGANIZATION NAME AND ADDRESS MECHANICAL & AEROSPACE ENGINEERING DEPARTMENT PRINCETON UNIVERSITY PRINCETON, NJ 08544		10. PROGRAM ELEMENT, PROJECT, TASK AREA & WORK UNIT NUMBERS 61102F 2308/A2
11. CONTROLLING OFFICE NAME AND ADDRESS AIR FORCE OFFICE OF SCIENTIFIC RESEARCH/NA BOLLING AFB, DC 20332		12. REPORT DATE August 1981 13. NUMBER OF PAGES 60
14. MONITORING AGENCY NAME & ADDRESS(if different from Controlling Office)		15. SECURITY CLASS. (of this report) UNCLASSIFIED 15a. DECLASSIFICATION/DOWNGRADING SCHEDULE

16. DISTRIBUTION STATEMENT (of this Report)

Approved for Public Release; Distribution Unlimited.

17. DISTRIBUTION STATEMENT (of the abstract entered in Block 20, if different from Report)

18. SUPPLEMENTARY NOTES

19. KEY WORDS (Continue on reverse side if necessary and identify by block number)

CATALYTIC COMBUSTION

20. ABSTRACT (Continue on reverse side if necessary and identify by block number)

Measurements of catalytic combustion of lean mixtures of propane/air at atmospheric pressure over platinum/alumina/cordierite catalysts were carried out over a broad range of equivalence ratios and flow velocities. Substrate (honeycomb) temperatures, chemical species at the catalyst were measured. A substantial data base for catalytic oxidation C_3H_8 over palatinum catalysts was obtained. A two-dimentional model of the gas-phase oxidation of propane was developed. When the experimental wall temperature is used as the boundary condition

(cont'd on Part 2)

DD FORM 1 JAN 73 1473 EDITION OF 1 NOV 65 IS OBSOLETE

UNCLASSIFIED

82 08 25 109

SECURITY CLASSIFICATION OF THIS PAGE (When Data Entered)

for the gas-phase reactions; emissions predicted from the model agree well with measured values. From comparison with the experimental data, indications are that propane oxidation takes place via a three-step kinetic mechanism. Also form study of the relative importance of gas-phase vs surface oxidation, conclusions are that most of the propane is burnt in the gas-phase rather than at the catalytic wall and that the wall kinetics is slower than the gas diffusion transplant.

will be improved. Theoretical predictions will be made and compared with measurements of velocity, temperature, and concentrations within the boundary layer above the catalyst obtained by conventional and Raman, absorption and fluorescence laser techniques.

STATUS OF CATALYTIC COMBUSTION STUDY

During the period covered by this report, lean combustion of carbon monoxide in air and in inert/oxygen mixtures, and of propane in air was modeled, and the predictions were compared with the experimental data already obtained. A new catalyst material, integral with the substrate, was also designed and is in the process of being tested.

A. EXPERIMENTAL APPARATUS

The new experimental apparatus used to collect the data is shown in Fig. 1. With respect to the old test rig, described in the previous (6/1/79 - 5/31/80) Annual Technical Report, the following modifications have been made: a) an Ingersoll-Rand compressor has been installed that can be connected to the air feedline, substituting for the Atlas-Copco compressor. The maximum pressure can now be increased from 10 to 20 atm. b) A second air flowmeter in parallel with the first makes possible very accurate air flow readings in the low velocity range. c) A fourth heater in series with the three already existing was added to raise the maximum inlet temperature to $\sim 900^{\circ}K$. d) A sixteen-loop gas-sampling and storage valve controlled by its own microprocessor has been connected to the gas chromatograph. This valve can perform automatic sequential GC analysis of samples acquired during the course of experimental runs.

Operation of the apparatus is described below. Preheated air at a measured flowrate is supplied to a 690 mm long test section with 25.4 mm square channel. A catalyst is placed with its downstream end 90 mm from the test section outlet, and insulated from the wall by Fiberfrax paper. Details of the catalyst section are shown in Fig. 2. A fuel injector consisting of five 1.6 mm diameter tubes, each containing five 0.3 mm diameter holes, is located 440 mm from the catalyst inlet. A combination pitot tube and thermocouple is mounted 200 mm from the catalyst inlet. In addition to measuring gas velocity and temperature,

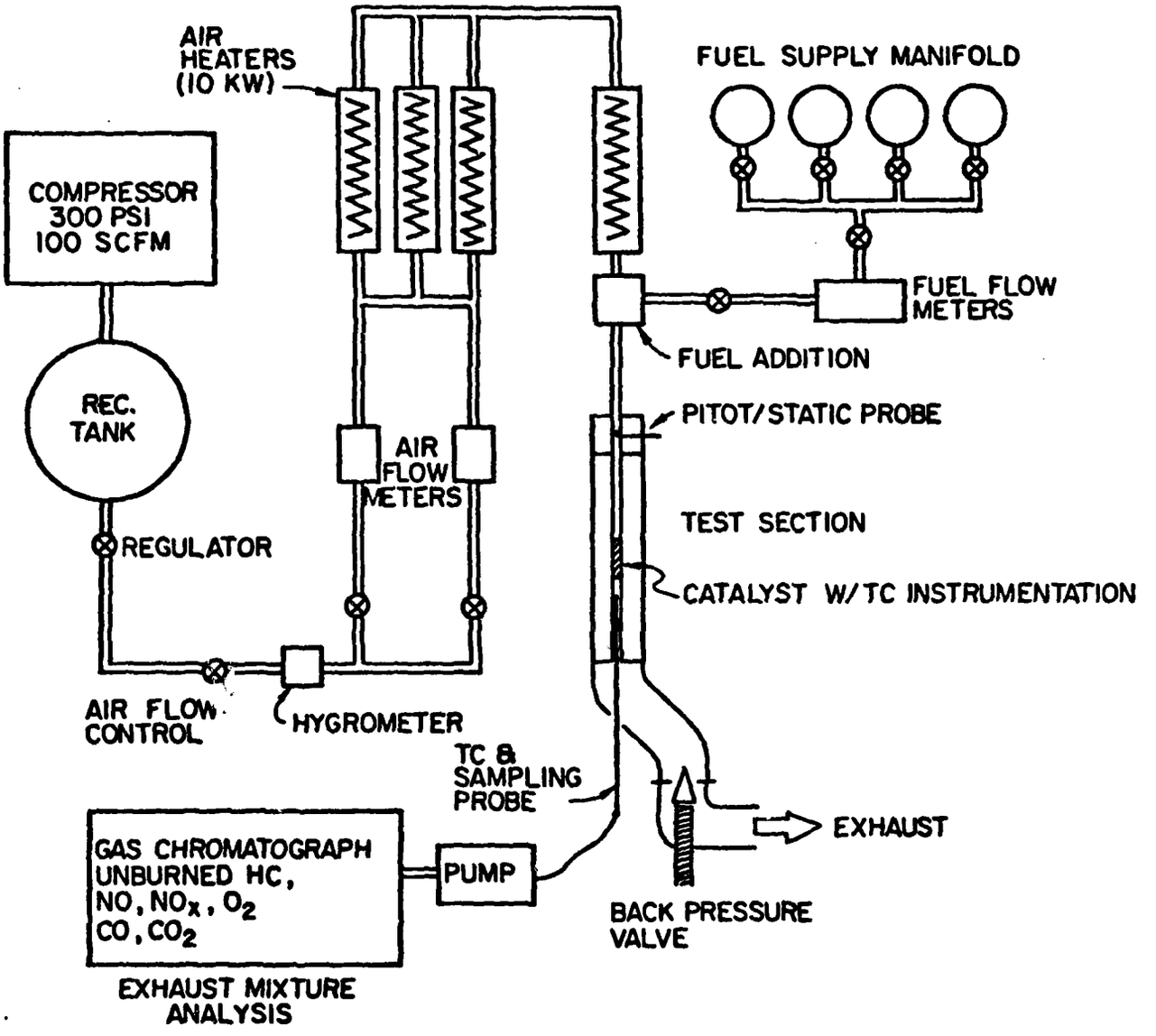

FIG. 1 CATALYTIC COMBUSTION FLOW SYSTEM

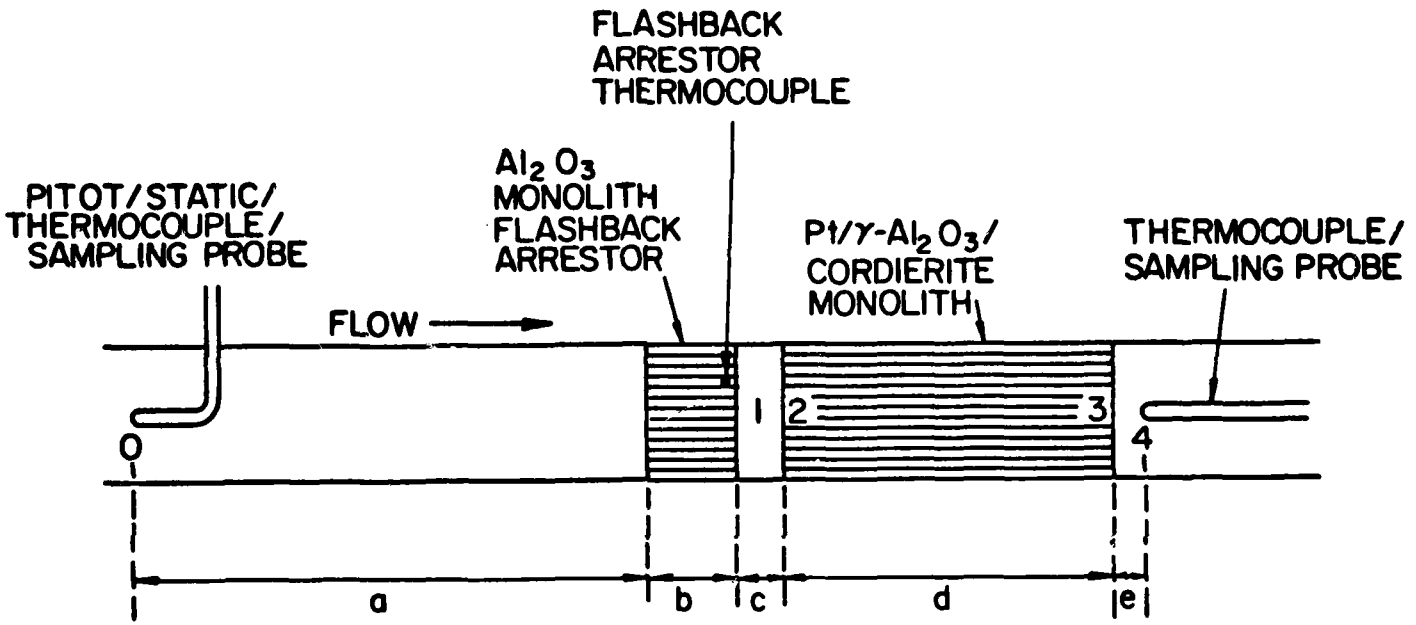

a 0.217 ± 0.001 m

b 0.0132 OR 0.0262 ± 0.0003 OR 0

c 0.001 TO 0.003

d 0.0760 ± 0.0003

e 0.0010 ± 0.0005

FIG. 2 DETAILS OF THE TEST SECTION

pitot tube is used to extract gas samples which are analyzed to determine equivalence ratio. Pressure is regulated by a valve in the exhaust pipe, and taps placed up and downstream of the catalyst are used to measure inlet pressure and pressure drop. A mass flowmeter (Hastings Model AHL-100P with H-3M/L-100 Transducer) measured the air flowrate. The water content of the inlet air was measured using a semiconductor sensor (Thunder Model 2000 with BR-101B probe) mounted in the airstream between the receiving tank and the heaters. Inlet conditions for the CO/air runs were the following:

Inlet temperature (T_{in}) = 600 ± 10 K
Inlet pressure (P_{in}) = 110 ± 5 kpa and 200 ± 7 kPa
Inlet velocity (u_{in}) = 10 ± 4 to 70 ± 9 m/s
CO/air equivalence ratio (ϕ) = 0.03 ± 0.006 to 0.32 ± 0.07
H_2O = 0.54 ± 0.007 mol%

For the C_3H_8/Air runs the inlet conditions were:

Inlet temperature (T_{in}) = 650 ± 13 K to 800 ± 16 K
Inlet pressure (P_{in}) = 110 ± 5 kPa
Inlet velocity (u_{in}) = 10 ± 4 to 40 ± 7 m/s
C_3H_8/air equivalence ratio (ϕ) = .19 ± .03 to .32 ± .04
H_2O = 1.2 ± .6 to 1.7 ± .6 mol%

A continuous effort has been made to minimize crosswise gradients in temperature, velocity, and fuel concentration of the inlet stream. The entire test section is insulated so that uniform temperature across the width of the test section is obtained when sufficient time (~1 hr) has elapsed after startup of the air preheat system. The uniformity is independent of the air flowrate over the range of velocities used. Sufficient fuel/air mixing was obtained only by placing screens downstream of the fuel injector, and these affect the velocity profile. By trying various configurations, the velocity uniformity was improved while maintaining an even distribution of fuel. The arrangement used in the present experiments consisted of two screens, each containing four 8 mm diameter holes, placed 30 and 110 mm downstream of the fuel injector. Another screen

perforated with 1.6 mm diameter holes was 190 mm from the injector and 50 mm upstream of the pitot tube. The resulting fuel distribution shows good uniformity (±3%) over the measured range. Velocity profiles are less satisfactory (range ±6% over 50% of the channel width). Average reference velocities were determined using the CO and air flowrates, inlet temperature and pressure, and the cross section area of the catalyst. The catalyst inlet velocity, taking into account the fraction of open monolith area, is $u_{in} = (1.67 \pm .06)u_{ref}$.

Substrate temperatures were measured by a method similar to that described by Kesselring, Krill, and Kendall (1977). Ni-Cr/Ni-Al thermocouples are fed through the test section wall and into the ends of catalyst channels. The lengths of wire inside the catalyst are covered by mullite insulator and both ends of the channel sealed with ceramic adhesive. The lifetime of these thermocouples under test conditions is short (5 - 20 hr). Exhaust gas samples were taken through an expansion quenched, water cooled, stainless steel probe mounted in an elbow downstream of the test section. Exhaust gas temperature was measured with a thermocouple mounted on the probe. CO and CO_2 were determined by infrared absorption (Horiba Model AIA-21), O_2 by magnetic susceptibility (Scott Model 250), and total hydrocarbon (HC, reported here as C_3) by a flame ionization detector (Scott Model 415).

The catalyst was platinum supported on split cell corrugated Cordierite with γ-alumina washcoat. The overall dimensions of the monolith were 24 x 24 x 76 mm, the open area was 64%, the channel cross-section area was 1.9 mm^2, and the platinum loading was 4.2 kg/m^3. The physical properties of the catalyst are listed in Table 1. The sample was pretreated by burning propane for two hours with the maximum substrate temperature at 1480K. The fuels were carbon monoxide, C.P. 99.5 mole% min, and natural propane, 96 mole%, nominal.

Table 1. Catalyst Properties

SUBSTRATE: Cordierite, American Lava Corp., AlSiMag 795, split cell

length 0.0760 ± 0.0003 m
wall thickness 0.25×10^{-3} m
open area 64%
channels per unit area 0.34×10^{6} m^{-2}
open area per channel 1.9×10^{-6} m^2
ratio surface area to total volume 2100 m^2/m^3
ratio surface area to gas volume 3260 m^2/m^3
channel hydraulic diameter (4/3260) 0.00123 m
bulk density 610 kg/m^3
solid density 1700 kg/m^3
safe operating temperature 1473K
specific heat 800 J/kg·K
coefficient of thermal expansion (linear, 294-1033K) 3.8×10^{-6} K^{-1}
thermal conductivity of solid (572K) 1.4 J/m·s·K

approximate channel cross-section is a trapezoid with base lengths .001m and .0023m, and height .0012m

WASHCOAT: γ-alumina

loading 115-125 kg/m^3
surface area (BET) $(29.2\text{-}33.0) \times 10^{6}$ m^2/m^3

CATALYST: platinum

loading 4.2 kg/m^3
surface area (CO chemisorption) 6×10^{4} m^2/m^3

The γ-alumina and platinum were applied by Matthey Bishop, Inc., Malvern, Pennsylvania.

B. MATHEMATICAL MODEL

For simplicity only an individual channel of the catalytic monolith was modeled. This assumes that in the radial, or crosswise direction, the temperature distribution inside the substrate is symmetrical, so that heat transfer between adjacent channels can be neglected. In actuality insulation of the monolith and of the test section limits crosswise gradients to ∿6 K/mm, or ∿10 K/channel. Since the embedded thermocouples and the combination thermocouple/sample probe measure quantities related to the central channels, errors due to nonuniform channel performance were minimal. Axisymmetry was assumed in modeling the individual channel, whose cross-section is roughly trapezoidal. The diameter of the model channel was chosen as the hydraulic diameter $D_h = \frac{2 \times \text{Area}}{\text{perimeter}}$. For the monolith used in this study D_h = 1.4 mm.

The gas-phase solution inside an individual monolith channel is based on the TEACH code documented by Gosman and Ideriah (1976). The general conservation equation is

$$\frac{\partial \rho\phi}{\partial t} + \frac{1}{r}\left[\frac{\partial}{\partial x}(\rho r u\phi) + \frac{\partial}{\partial r}(\rho r v\phi) - \frac{\partial}{\partial x}\left(r\Gamma \frac{\partial \phi}{\partial x}\right) - \frac{\partial}{\partial r}\left(r\Gamma \frac{\partial \phi}{\partial r}\right)\right] = S_\phi$$

where $\phi \equiv u, v, T, Y_k$, etc.; Γ is the appropriate transport property, such as μ, κ, ρD_{ik}, and S_ϕ is the appropriate source term, such as $-\frac{\partial p}{\partial x}$, or the rate of formation for the species equations.

Molecular transport properties were used throughout the calculations, as the Reynolds number (based on inlet flow conditions) was, at most, ≈1900.

a) CO Chemical Kinetics Model

The model chosen for the gas-phase kinetics of CO with O_2 is a simple, one-step overall reaction $CO + \frac{1}{2} O_2 \rightarrow CO_2$. The rate was taken from Howard, Williams and Fine (1973):

$$\frac{d[CO]}{dt} = -K_o\,[CO][O_2]^{0.5}\,[H_2O]^{0.5}\,\exp(-E/RT)$$

with $K_o = 1.3 \times 10^{14}$ cm^3/mole·sec

$E = 126$ KJ/mole = 30 Kcal/mole

Justification for this model lies mainly in its simplicity.

The model for the catalytic wall assumes that the rate of CO oxidation at the wall is infinitely fast, i.e. that the CO concentration goes there to zero. This was later confirmed experimentally, and also is the only assumption that could reasonably reproduce the experimental emission data.

b) C_3H_8 Chemical Kinetics Model

In the gas phase a set of three overall reactions based on the Hautman model (1981) describes pyrolysis of C_3H_8 with formation of an intermediate (C_2H_4), oxidation of the intermediate to CO, and finally CO combustion to CO_2. The actual reaction rates in the present work are in the original form Hautman used initially to correlate his data (Hautman, 1980). The justification for choosing it is in its convenience: the rates stay always finite, while in the more recent form the inverse dependence of the C_2H_4 oxidation rate on C_3H_8 may result in an excessively large rate wherever C_3H_8 goes to zero. Because of the very nature of the numerical solution, this indeed may happen; to prevent this type of problem the old form for the rates was used. This did not change the corresponding rates at the average temperature of the gas inside the pipe.

The 3-step mechanism for propane oxidation in the gas phase was essential for a good agreement with the experimental data. (No reasonable results could be obtained by simply assuming C_3H_8 to break down into CO and then oxidizing CO to CO_2). At the platinum surface the same three fuel species present in the gas react to form products. Pyrolysis rates for propane are in fact much slower than diffusional or convection rates

for the geometry in question (Hautman et al, 1981). Evidence for the formation of lighter intermediates at the surface is scarce; however it is difficult to imagine a straight-chain hydrocarbon breaking all its C-H bonds simultaneously to form CO_2 and H_2O. In fact, lower temperature studies show that propane dehydrogenates to propene on Platinum (Biloen et al, 1977). It is therefore conceivable that formation of intermediates, and possibly radical species, take place very close to the catalyst, i.e. in a thin sublayer embedded in the channel boundary layer. If so, only optical techniques could detect them.

In order to simplify the model both conceptually and numerically, the assumption was made of one-step reactions at the catalytic wall. Heterogeneous rates data were obtained from Schwartz et al (1971). As for CO, infinitely-fast kinetics was assumed. With these assumptions, the reactions and their rates are shown in Table 2.

To test the validity of the model and separate gas phase effects from substrate effects, the gas phase equations were solved by uncoupling them from the substrate energy equation. In this case the only extra unknown variable is the wall temperature, which was taken from the experiments and imposed as boundary condition at the wall. This procedure has as advantage the implicit inclusion of radiative effects in the model (provided the gas is optically thin), since the experimental wall temperature does include the effects of radiation.

C. RESULTS

a) CO/Air Mixtures

A total of 78 runs were performed. Analysis of the $\Delta p/p$ results indicates that the hydrulic diameter choice $2R = 1.4$ mm in the model reproduces the experimental data (within the error limits) at both $p = 110$ and $p = 200$ kPa. Trends are as expected, with $\Delta p/p$ increasing with velocity and ϕ (i.e. gas temperature)

TABLE II. CHEMICAL REACTION RATE DATA USED IN THE MODELING OF 3-STEP KINETICS OR PROPANE OXIDATION ON $Pt/\gamma\text{-}Al_2O_3$/CORDIERITE CATALYST

REACTIONS

	GAS	WALL
1.	$C_3H_8 + \frac{1}{2} O_2 \rightarrow \frac{3}{2} C_2H_4 + H_2O$	$C_3H_8 + 5O_2 \rightarrow 3CO_2 + 4H_2O$
2.	$C_2H_4 + 2O_2 \rightarrow 2CO + 2H_2O$	$C_2H_4 + 3O_2 \rightarrow 2CO_2 + 2H_2O$
3.	$CO + \frac{1}{2} O_2 \rightarrow CO_2$	$CO + \frac{1}{2} O_2 \rightarrow CO_2$

RATES

	GAS (mol/cm^3·s)	WALL (mol/cm^2·s)
1.	$-1.4 \times 10^9 \exp(-40608/RT)$ $\cdot ([C_3H_8]/[C_3H_8]_{in})^{.25} [O_2]^{1.04}$	$-1.51 \times 10^3 \exp(-17600/RT) [C_3H_8]$
2.	$-6.15 \times 10^{13} \exp(-60184/RT)$ $\cdot ([C_2H_4]/[C_3H_8]_{in})^{.96} [O_2]^{1.18}$	$-80 \exp(-12000/RT)[C_2H_4]$
3.	$-2.2 \times 10^{12} \exp(-40000/RT)$ $\cdot [CO][O_2]^{.25}[H_2O]^{.5}$	$-3.83 \times 10^3 \exp(-24900/RT)$ $[CO]$

since $\Delta p/p$ grows with both viscosity and velocity gradient at the wall (see Figs. 3 and 4). A sample of wall temperature profiles is shown in Figs. 5, 6 and 7. At the same equivalence ratio there is hardly any effect due to velocity or pressure, meaning that the overall heat release process is diffusion-controlled. Flow velocity does not affect heat release at the wall since it does not affect CO diffusional transport rate; as for pressure, the reduction in diffusional transport at higher pressures is compensated by the reduction in thermodiffusivity $\alpha = k/C\rho\rho$, provided of course that Le $\simeq$ 1.

Emissions in terms of $\xi = X_{CO}/(X_{CO} + X_{CO_2})$ i.e. in terms of unburnt carbon, are plotted versus ϕ in Figs. 8 and 9. The theoretical model predicts emissions well at high and intermediate velocities while is less satisfactory when the velocity is low. The main features of CO combustion can be deduced from Fig. 8. At a constant flow velocity and $\phi = 0$, $X_{CO}/(X_{CO} + X_{CO_2})$ is unity. As ϕ is slightly increased, the catalytic reactions, slow because of $\phi \simeq 0$, tend to reduce CO, and emissions drop. This regime, in which only part of the CO transported at the wall by diffusion is catalytically oxidized is the kinetically-controlled regime, where finite CO conversion rates (of the type suggested by Voltz et al. in 1973) apply.

Still increasing ϕ accelerates the wall reaction(s) until they become as fast, or faster, than the rate of transport to the wall. At this point the regime becomes diffusion-controlled which is shown by an invariance with respect to ϕ. This flat part of the emission curves is broader at higher flow velocities (short residence time) and becomes very narrow, i.e. barely noticeable, for long residence times.

Eventually, as ϕ is further increased and the wall becomes hotter, gas-phase chemical reactions become faster and more and more CO is oxidized in the gas phase, bringing down emissions.

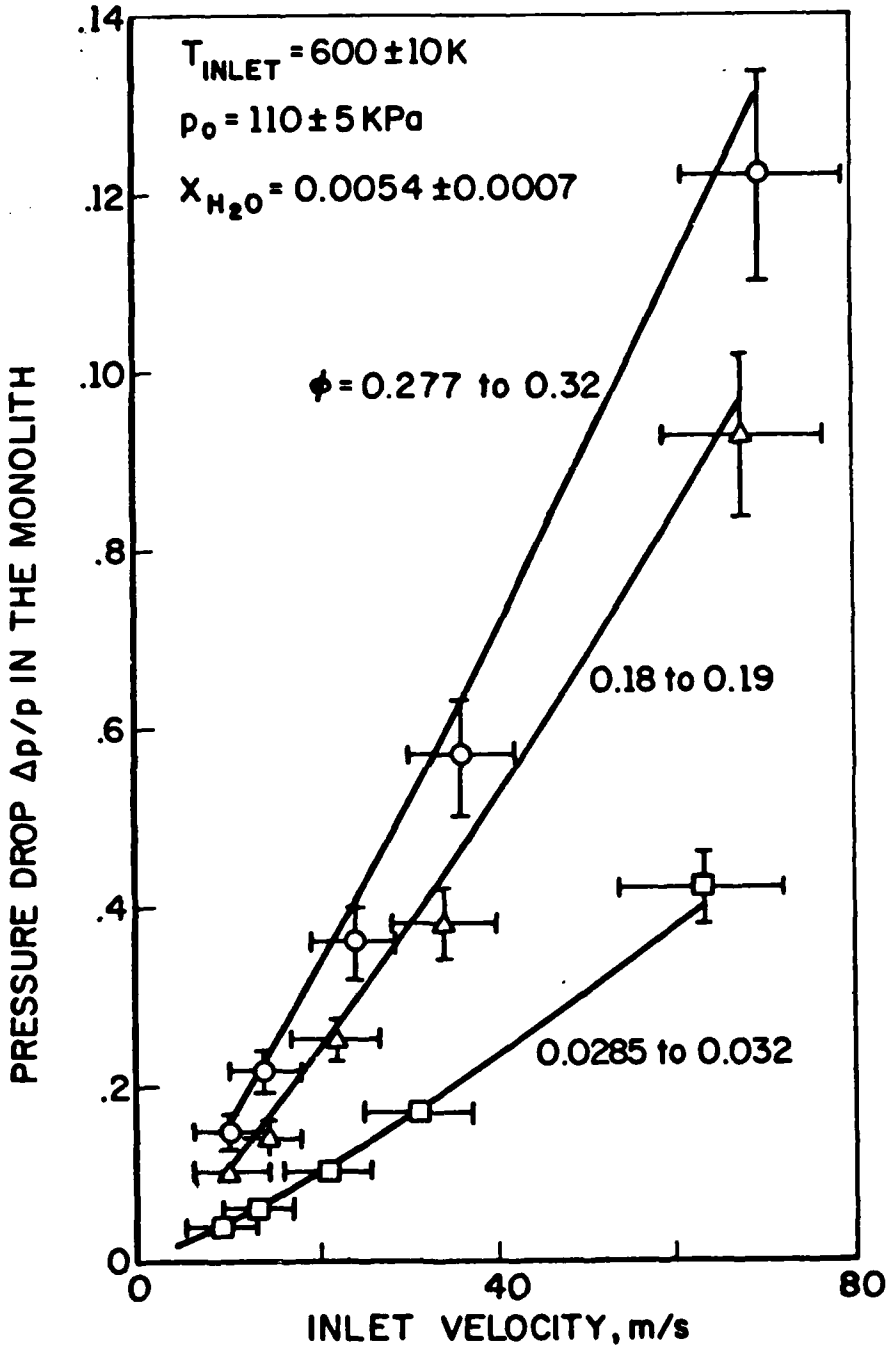

FIG. 3. Pressure Drop Inside the Monolith As a Function of Inlet Parameters for CO/Air Oxidation on Pt.

P_0: △ 110±5 KP_a
○ 200±7 KP_a
T_0 = 600±10 K
$\langle U_2 \rangle$ = 22±5 m/s

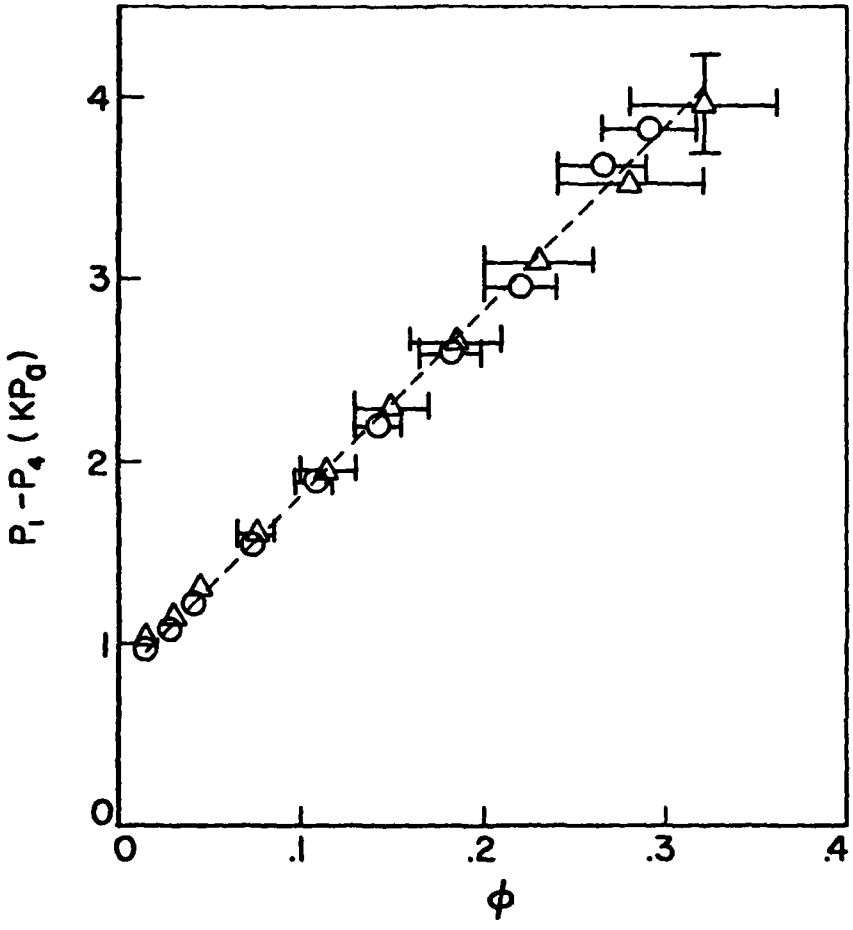

FIG. 4. PRESSURE DROP vs. EQUIVALENCE RATIO
- - - - Theoretical predictions

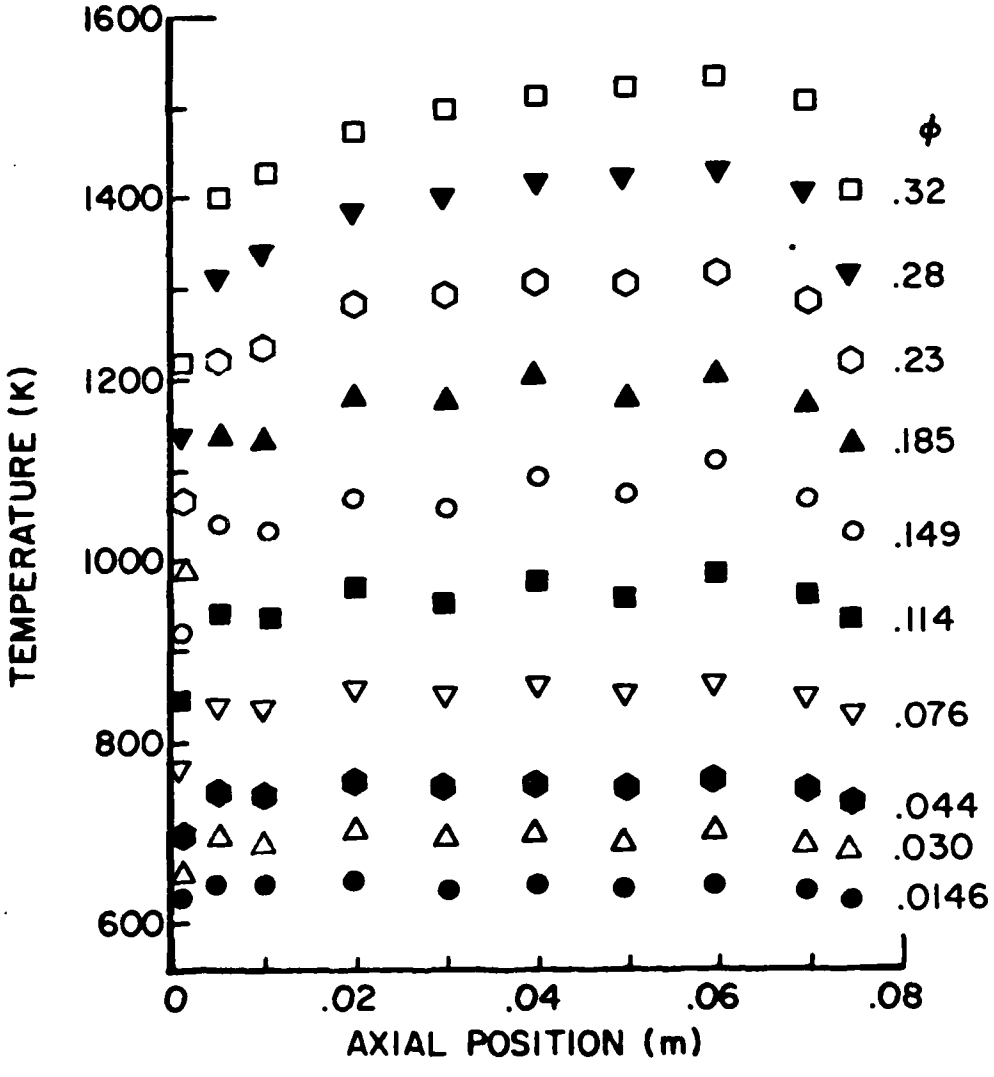

FIG. 5 SOLID TEMPERATURE - CO COMBUSTION

$\dot{m}_{AIR} = .0038$ kg/s

$U_{INLET} = 22.1 \pm 2.6$ m/s

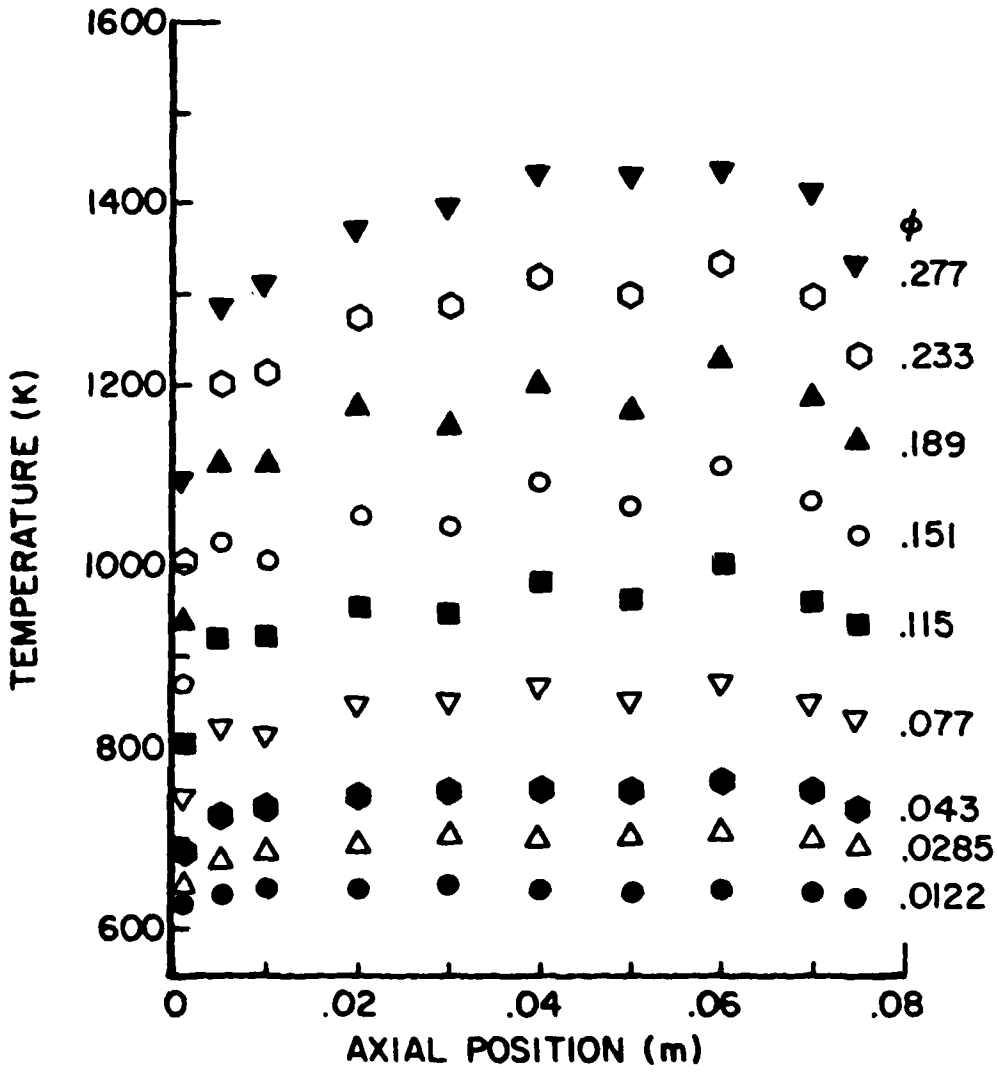

FIG. 6 SOLID TEMPERATURE – CO COMBUSTION

$\dot{m}_{AIR}$ = .0114 kg/s

U_{INLET} = 66 ± 7 m/s

$P_0 = 200 \pm 7$ KPa
$T_0 = 600 \pm 10$ K
$\langle U_z \rangle = 22 \pm 4$ m/s

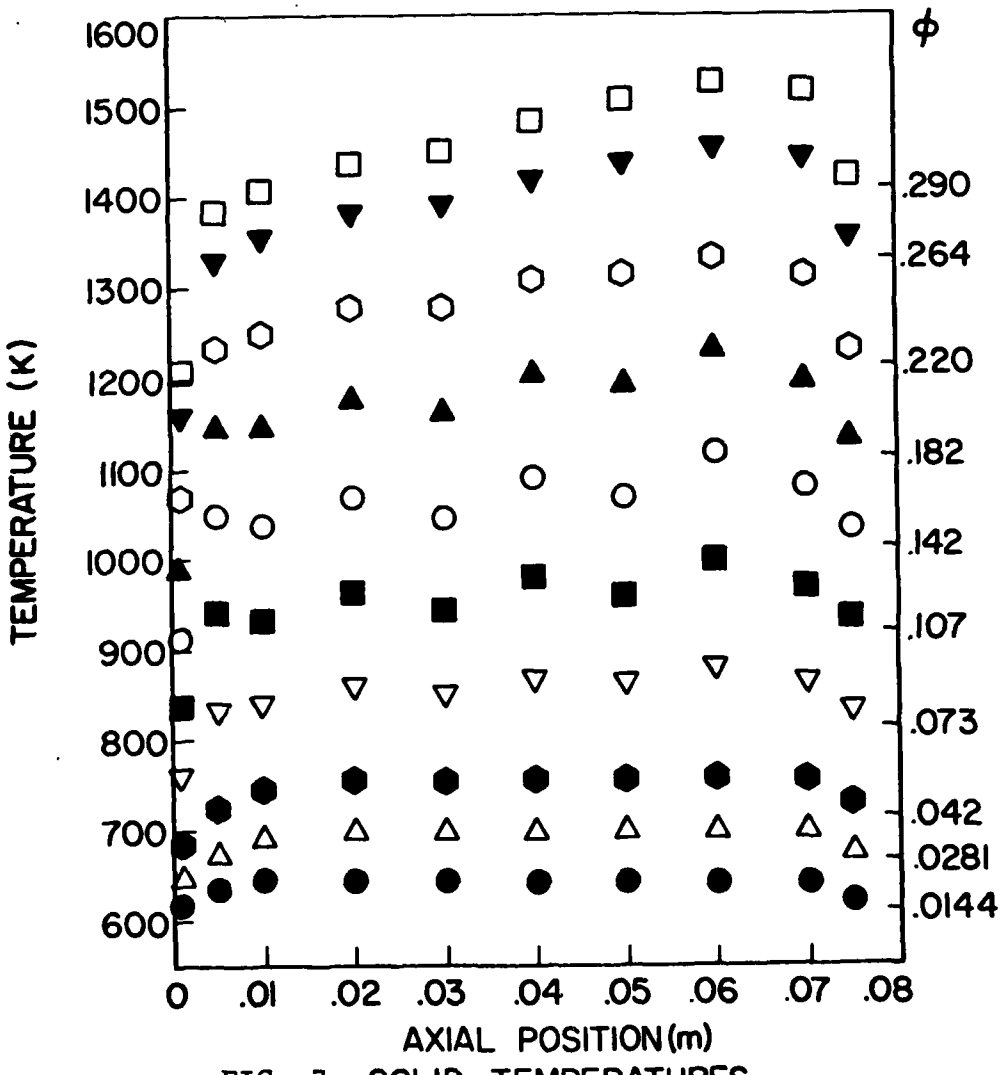

FIG. 7 SOLID TEMPERATURES
CO/AIR COMBUSTION

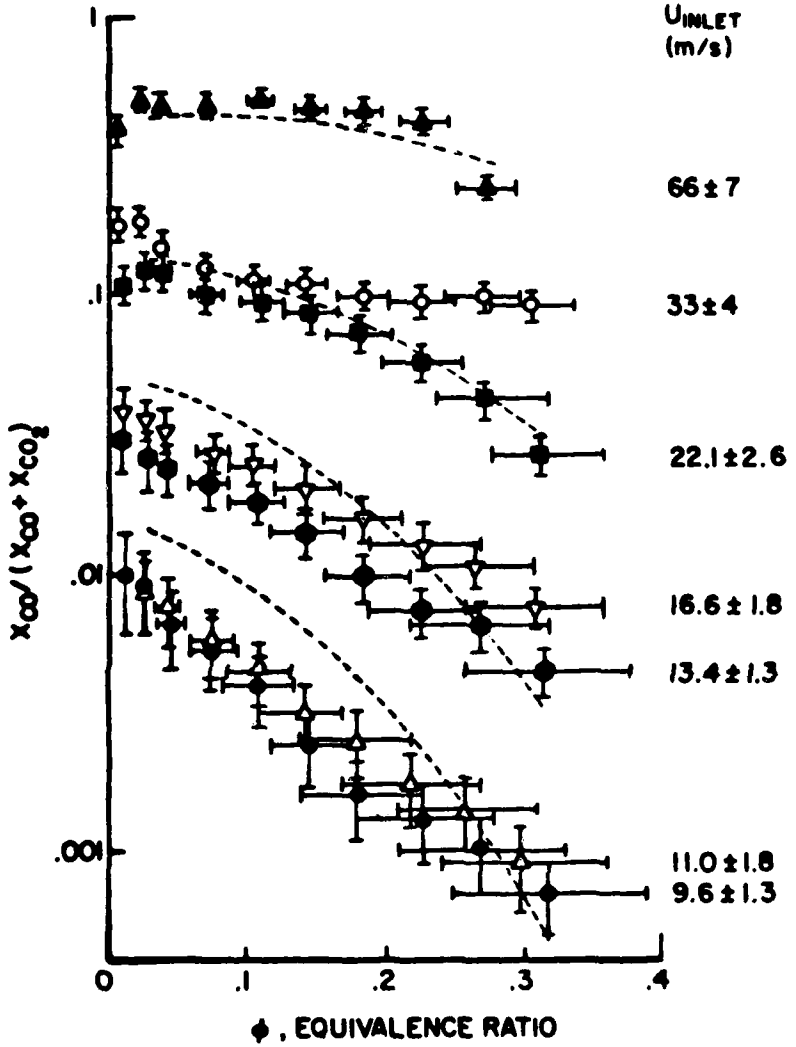

FRACTION OF CO UNBURNED VS EQUIVALENCE RATIO

(DATA WERE TAKEN IN THE FOLLOWING CONSECUTIVE ORDER)

$\Delta\nabla o\blacktriangle\blacksquare\bullet\bullet$

---------- THEORETICAL PREDICTIONS

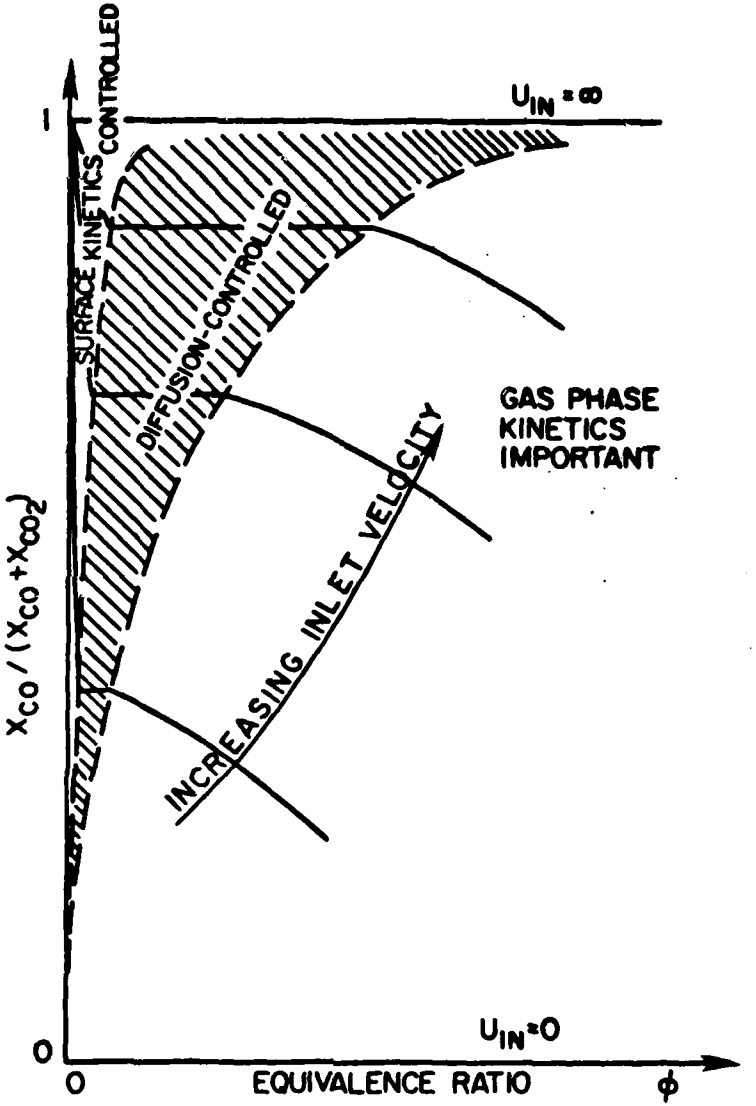

CONCEPTUAL UNDERSTANDING OF CO OXIDATION ON PLATINUM

FIG. 8. COMPARISON OF THEORETICAL AND EXPERIMENTAL RESULTS: CO OXIDATION

Increasing or reducing the flow velocity alters quantitatively but not qualitatively this conceptual description. In particular, the emission plateau corresponding to the pure diffusion-controlled regime is very narrow at low velocities and broadens as the velocity is increased, until, when the velocity is infinitely large, occupies the entire ϕ range, i.e. $X_{CO}/(X_{CO} + X_{CO_2}) = 1$.

The effect of pressure can be observed in Fig. 9. Since the diffusion coefficients are inversely proportional to pressure, increasing p from 110 to 200 kPa raises emissions and widens the purely diffusion-controlled region. For $\phi \gtrsim .3$ the experimental data show a steeper slope for p = 200 kPa. This is again the effect of gas-phase kinetics, which is roughly proportional to p^2, thus favoring emission reductions when the pressure is raised.

The theoretical model underpredicts emissions at larger ϕ and for longer residence times, i.e. when gas-phase kinetics contributes substantially to CO conversion. This observation leads to suspect the overall, one-step CO oxidation rate of Howard et al. The rate was proposed for lean CO/air reactions at p = 1 atm., and may not be applicable to higher pressures and larger ϕ.

An important question for practical applications of catalytic combustion concerns the relative magnitude of gas-phase versus wall CO oxidation.

Figure 10 shows that gas phase becomes important for CO conversion only toward the outlet of the channel, where temperature also is highest. Integrating the local wall and gas-phase contribution over the entire channel gives the overall effect of the catalyst, which is dominant at high velocities and lower ϕ. When residence time is lengthened and ϕ is higher gas-phase CO conversion is no longer negligible (Fig. 11).

$T_0 = 600 \pm 10$ K

$\langle U_2 \rangle = 22 \pm 5$ m/s

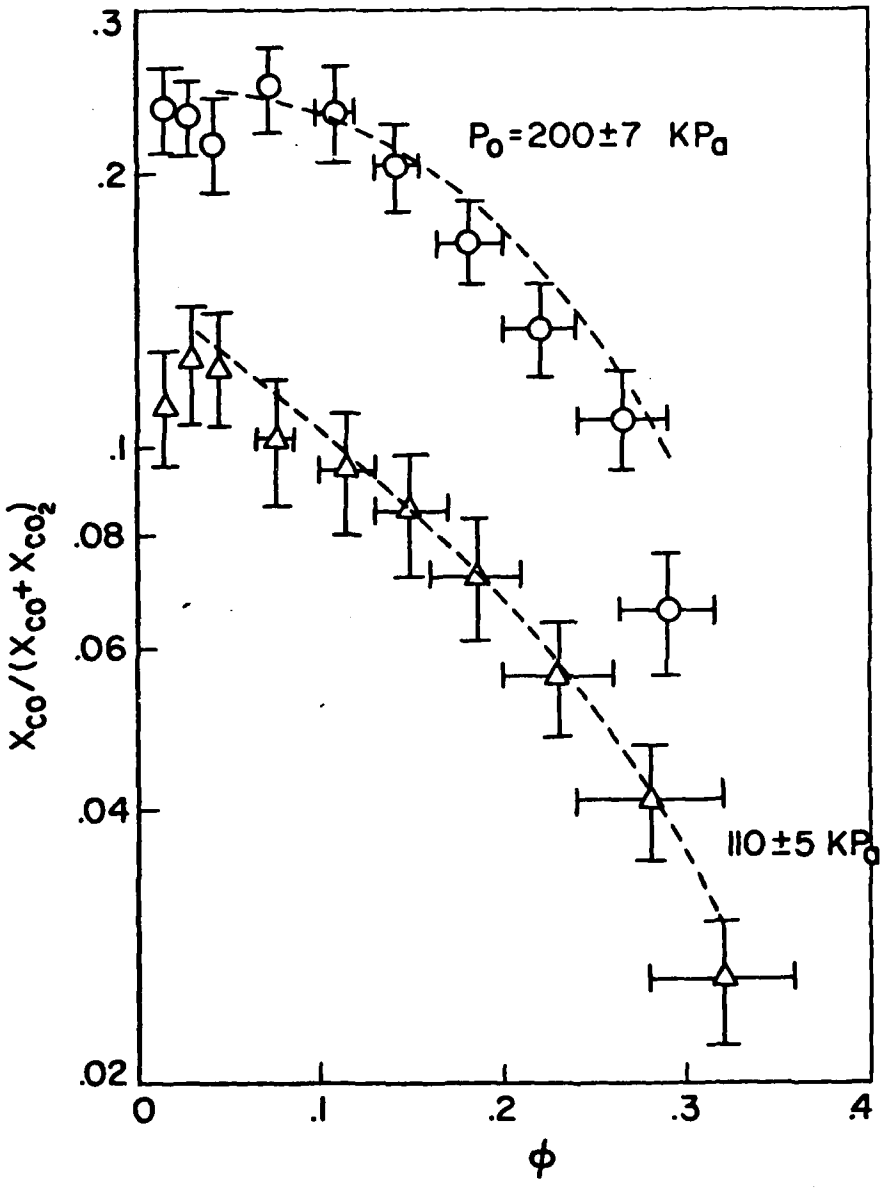

FIG. 9. FRACTION OF CO UNBURNED vs EQUIVALENCE RATIO

--- Theory

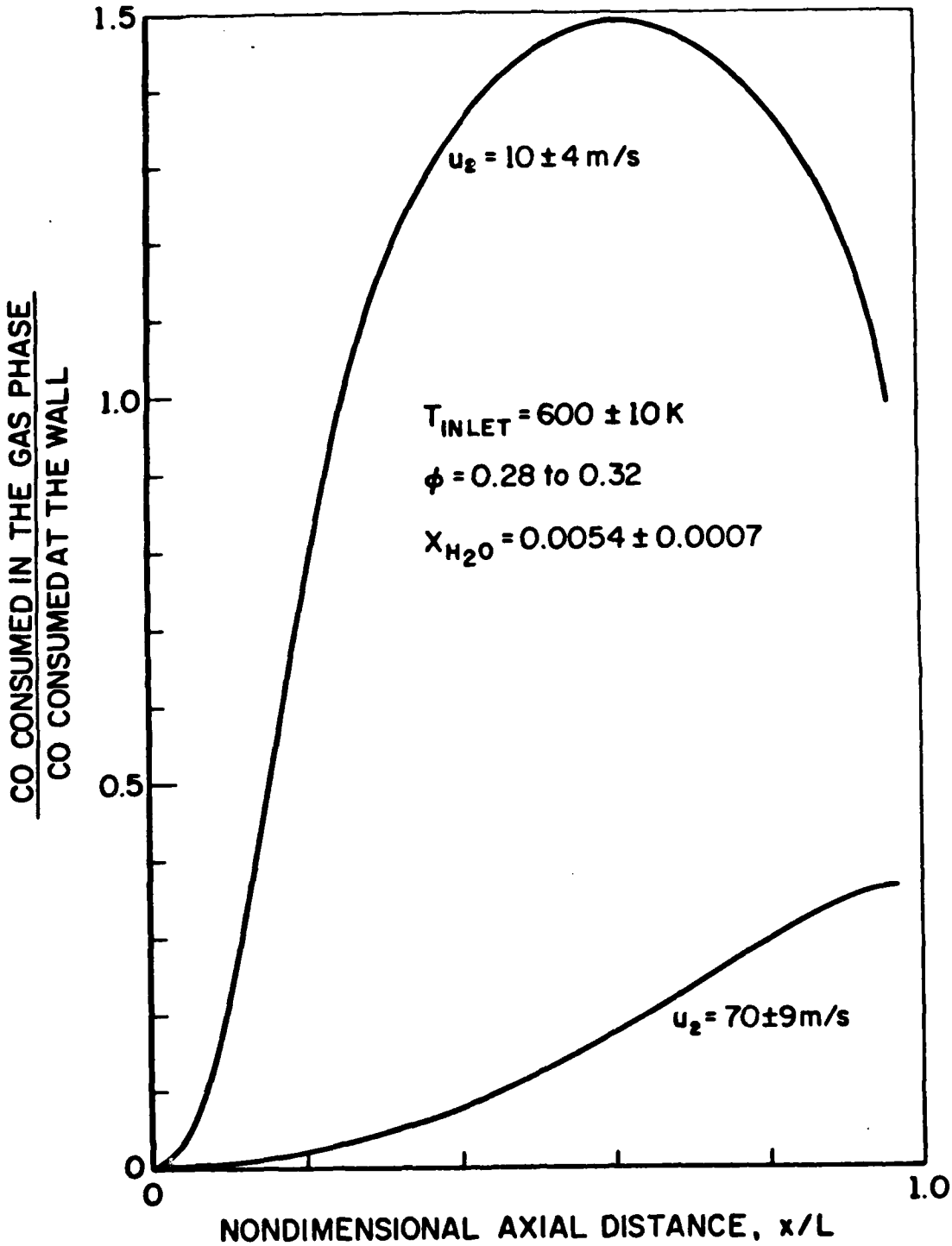

FIG. 10A. Gas Phase vs. Surface Contribution to CO/Air Oxidation on Pt-Effect of Velocity

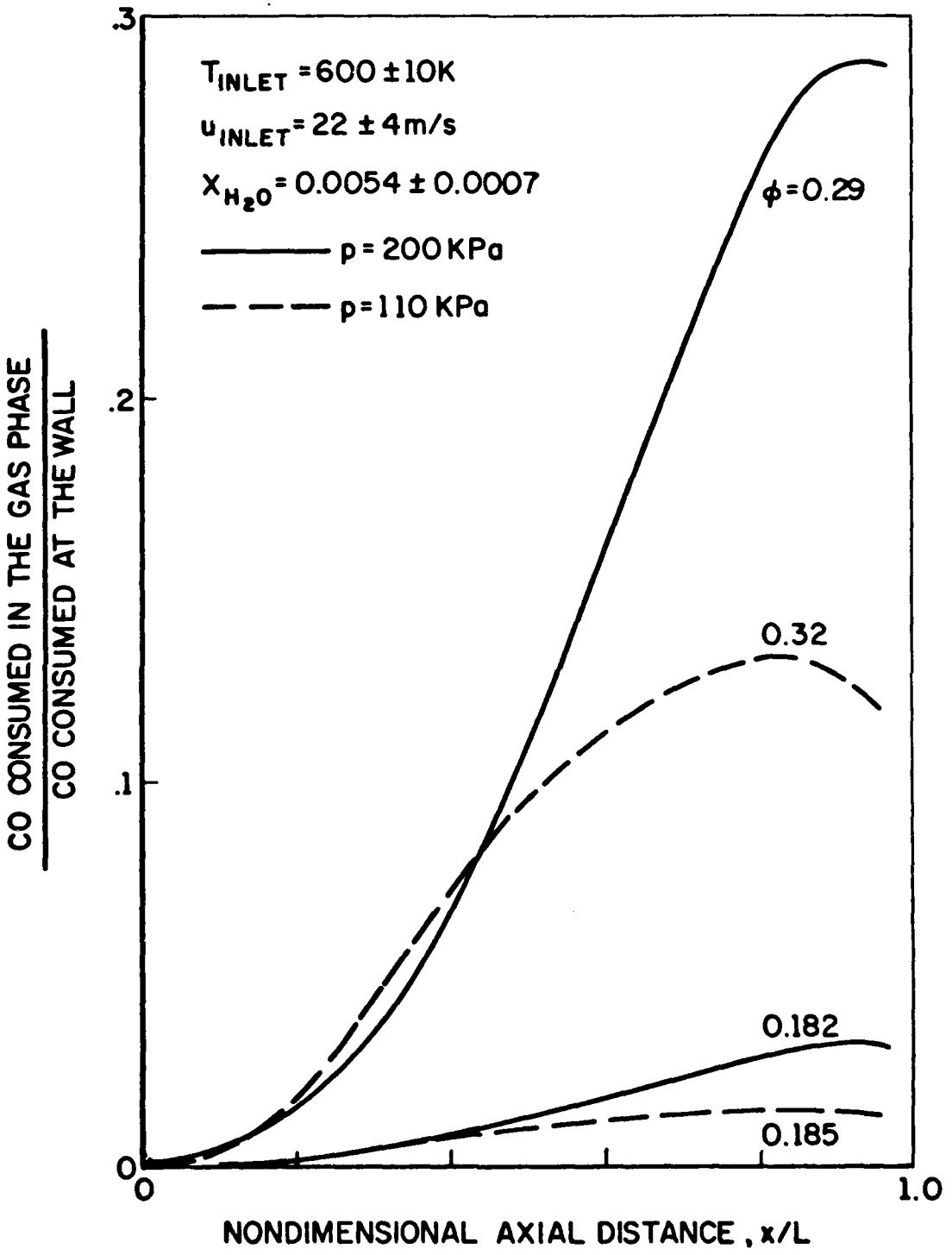

FIG. 10B. Gas Phase vs. Surface Contribution to CO/Air Oxidation on Pt-Effect of ϕ and Pressure

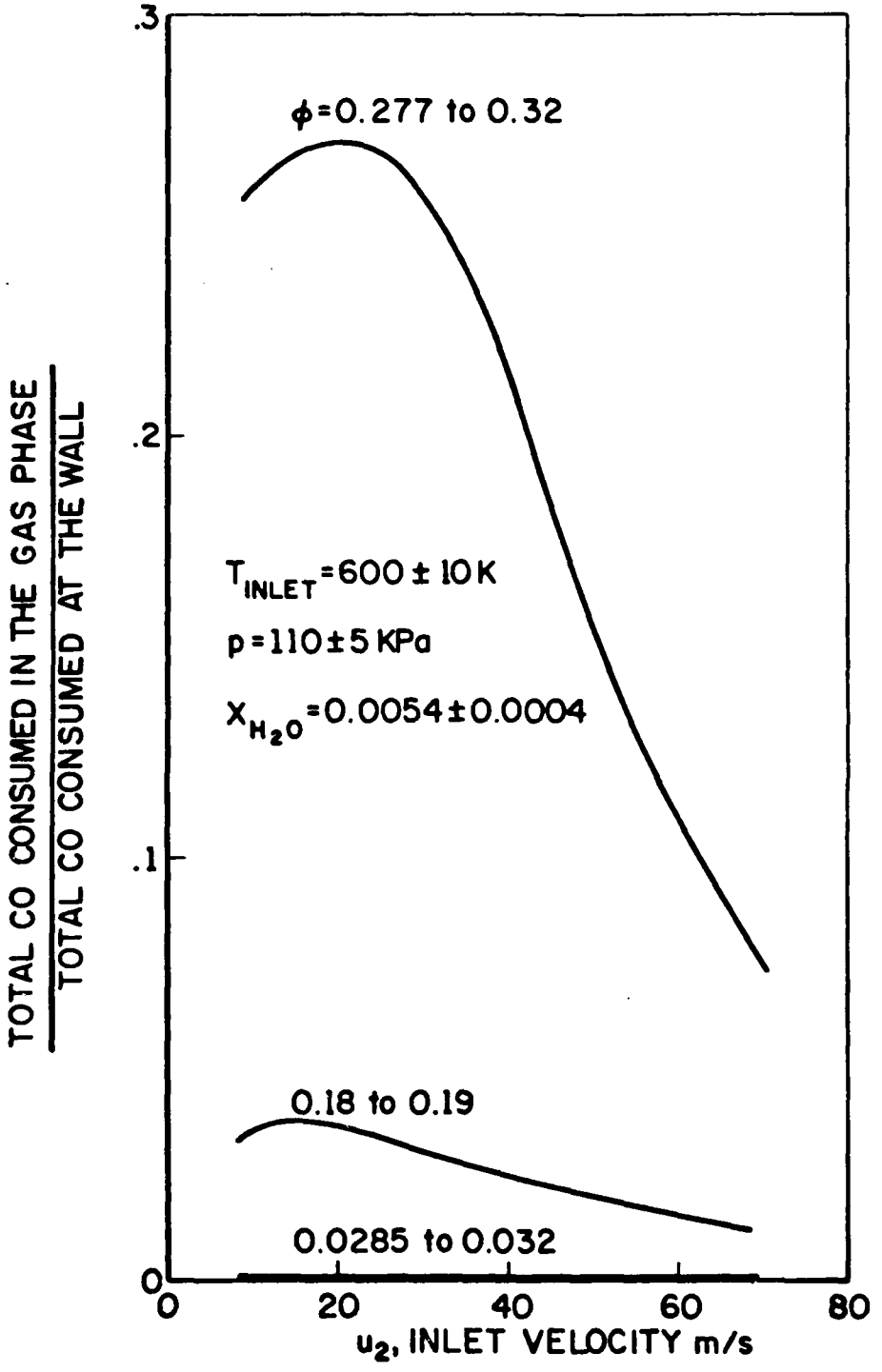

FIG. 11A. Gas Phase vs. Surface Contribution to CO/Air Oxidation on Pt - Effect of ϕ and Velocity

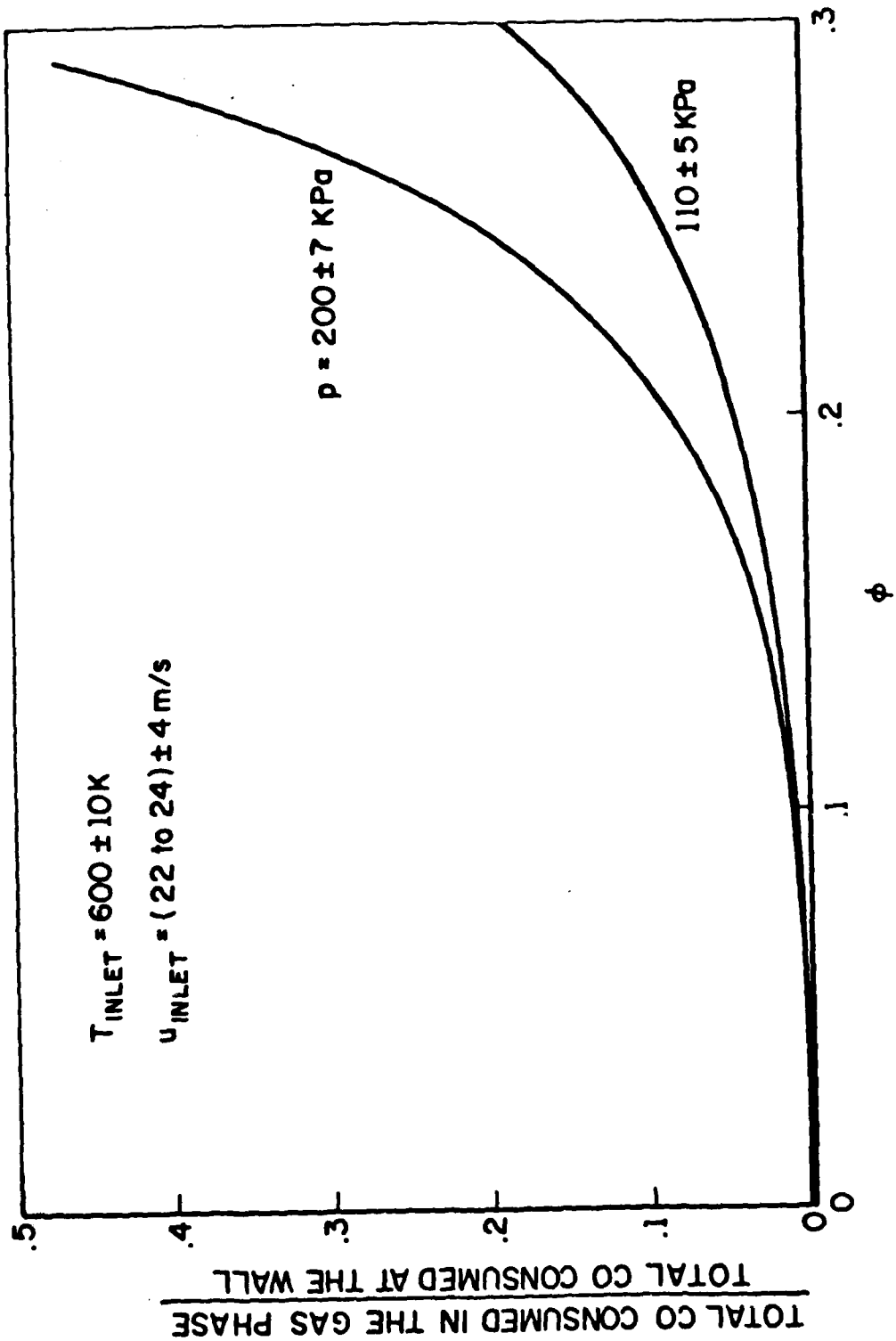

FIG. 11B. Gas Phase vs. Surface Contribution to Co/Air Oxidation on Pt - Effect of ϕ and Pressure

b) CO/Inert/O_2 Mixtures

To verify the effect of diffusion on CO conversion a total of 51 runs were performed with fuel/oxidizer combinations in which air was replaced by mixtures of an inert (N_2, CO_2, He, A) and O_2. The experimental procedure in these runs consisted in bringing the temperature of the test section and connected hardware to the desired steady-state conditions using ambient air from the compressor, switching to the CO/Inert/O_2 mixture for the actual data taking.

The influence of diffusion can be estimated in terms of the binary diffusion coefficient, which for a mixture of gases depend on the molecular weights of the individual components in a rather complex way. For simplicity, since the mass fraction of the inert gas dominates over all others, and since the molecular weights of CO and O_2 are similar, the effect of replacing N_2 by A, He or CO_2 may be studied by looking only at the change in the binary diffusion coefficient of CO and the inert gas.

For gas 1 ≡ CO and gas 2 ≡ inert, the ratio $D_{1,2}/D_{1,N_2}$ is:

Inert Gas 2	$D_{1,2}/D_{1,N_2}$
CO_2	0.86
N_2	1.00
A	1.03
He	2.84

i.e. the mass transfer of CO in He should proceed approximately 2.8 times faster than for CO in nitrogen.

When the input parameters such as inlet temperature, velocity and equivalence ratio are kept unchanged and only the inert gas is varied, the results show only the effect of diffusive mass and heat transfer, since gas and surface kinetics are not directly affected by the presence of the inert gas.

With reference to the nomenclature in Fig. 2, the parameters and conditions kept fixed were:

Inert Gas:	A	He	N_2	CO_2	
Pressure p_o:	110±4	110±4	110±4	110±4	kPa
Inlet Temperature T_o:	600±10	700±20	700±10	690±14	K
Inlet Velocity u_2:	11±6	13±7	13±5	13±4	m/s
Stoich. Fuel/(O_2+Inert) ratio:	0.297	1.175	0.274	0.395	

CO conversion is illustrated in Figs. 12, 13 and 14. Fig. 12 shows the dependence on equivalence ratio for the case of CO_2 as an inert. Comparing the results with the ones for N_2, A and He in Figs. 13 and 14, it is clear that unburned CO increases, increasing the average molecular weight of the gas mixture.

Figs. 15 through 18 show the experimental measurements of substrate temperature versus axial position for the four inert gases tested and for various equivalence ratios. From these data is also clear that the average substrate temperature increases with the magnitude of the binary diffusion coefficient of the (CO/inert gas) mixture as can be seen from the following table:

Average Substrate Temperature, K

Inert Gas	CO_2	N_2	He
ϕ			
0.1	850	950	1050
0.2	1000	1200	1400
0.38	1250	1450	no data

The data on Argon are not included here since the lower inlete temperature makes unfair the comparison with the other three inert gas cases. No runs were attempted with He as the inert gas for $\phi > 0.25$, since the cordierite substrate could not

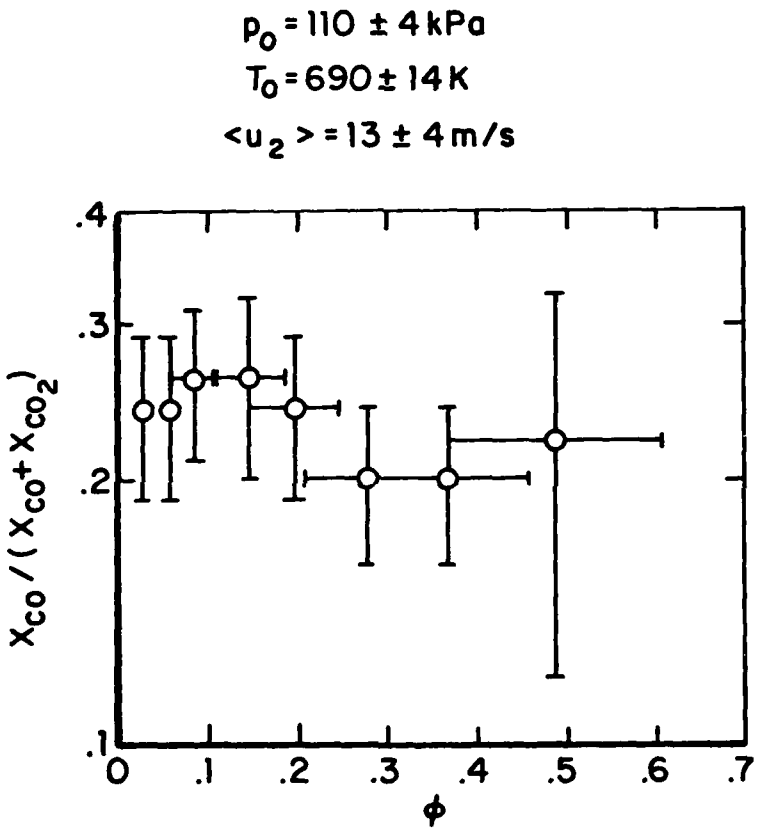

FIG. 12 FRACTION OF CO UNBURNED VS. EQUIVALENCE RATIO: $CO/O_2/CO_2$

$p_0 = 110 \pm 4$ kPa

$T_0 = 700 \pm 10$ K

$\langle u_2 \rangle = 13 \pm 5$ m/s

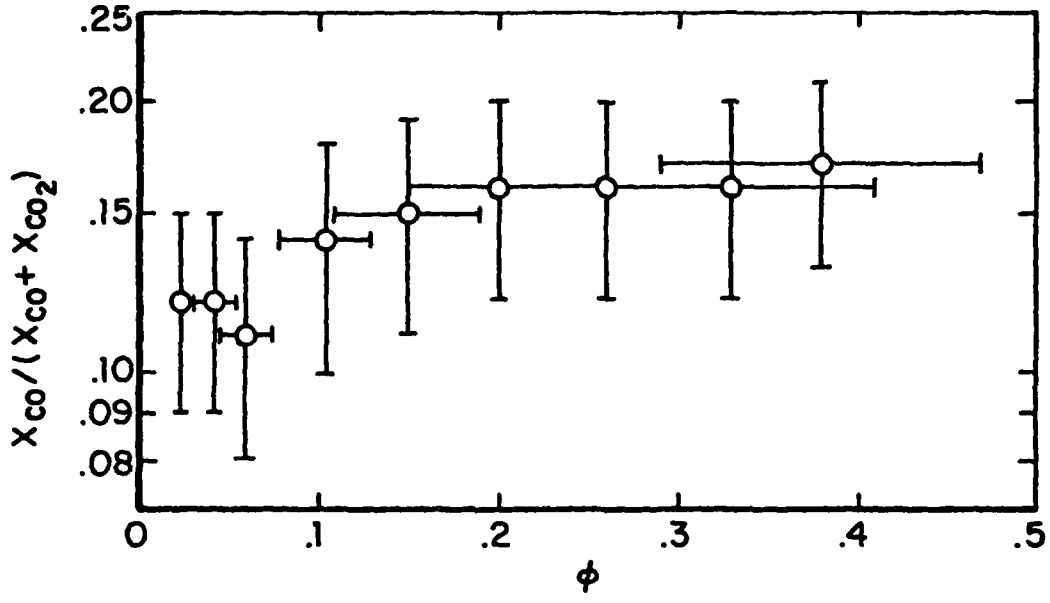

FIG. 13. FRACTION OF CO UNBURNED VS. EQUIVALENCE RATIO $CO/O_2/N_2$

Ar	He
$p_0 = 110 \pm 4$ kPa	110 ± 4 kPa
$T_0 = 600 \pm 10$ kPa	700 ± 20 K
$\langle u_2 \rangle = 11 \pm 6$ m/s	13 ± 7 m/s

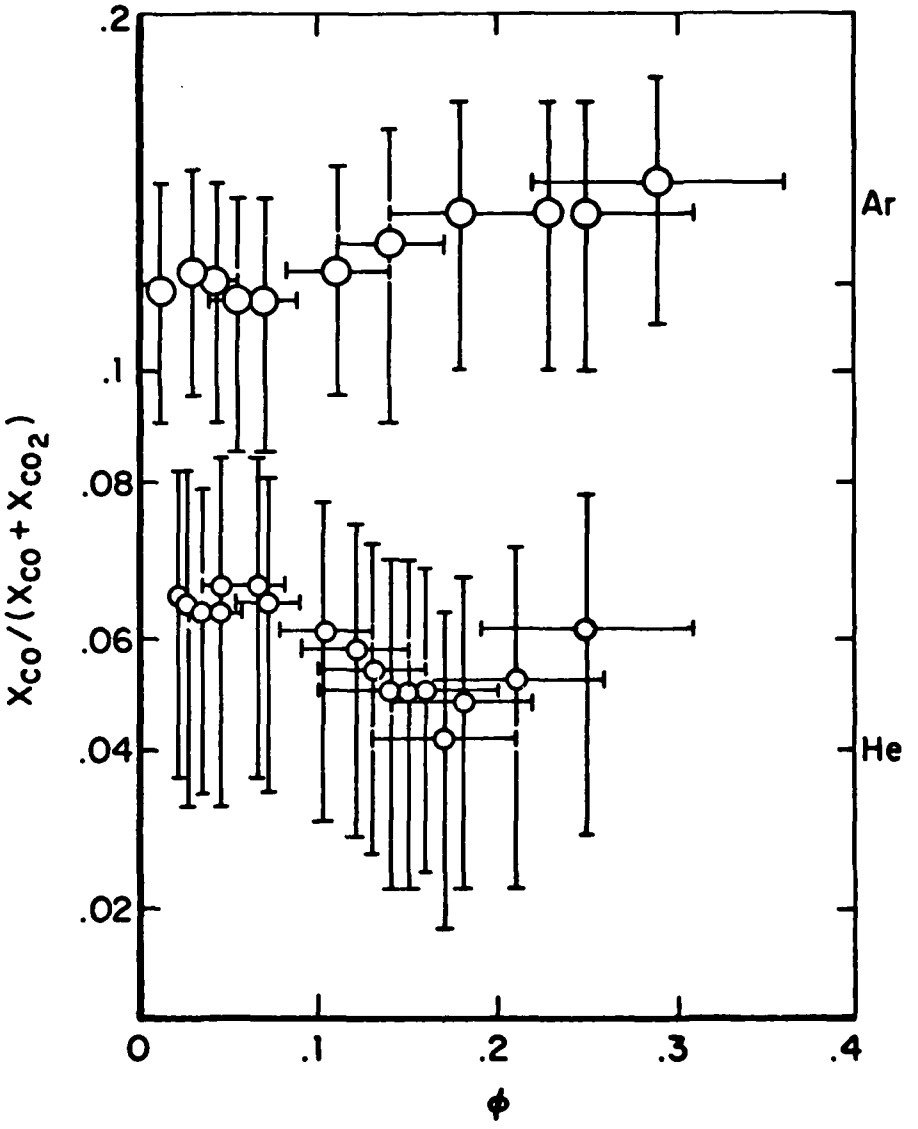

FIG. 14 FRACTION OF CO UNBURNED VS. EQUIVALENCE RATIO: $CO/O_2/Ar$ AND $CO/O_2/He$

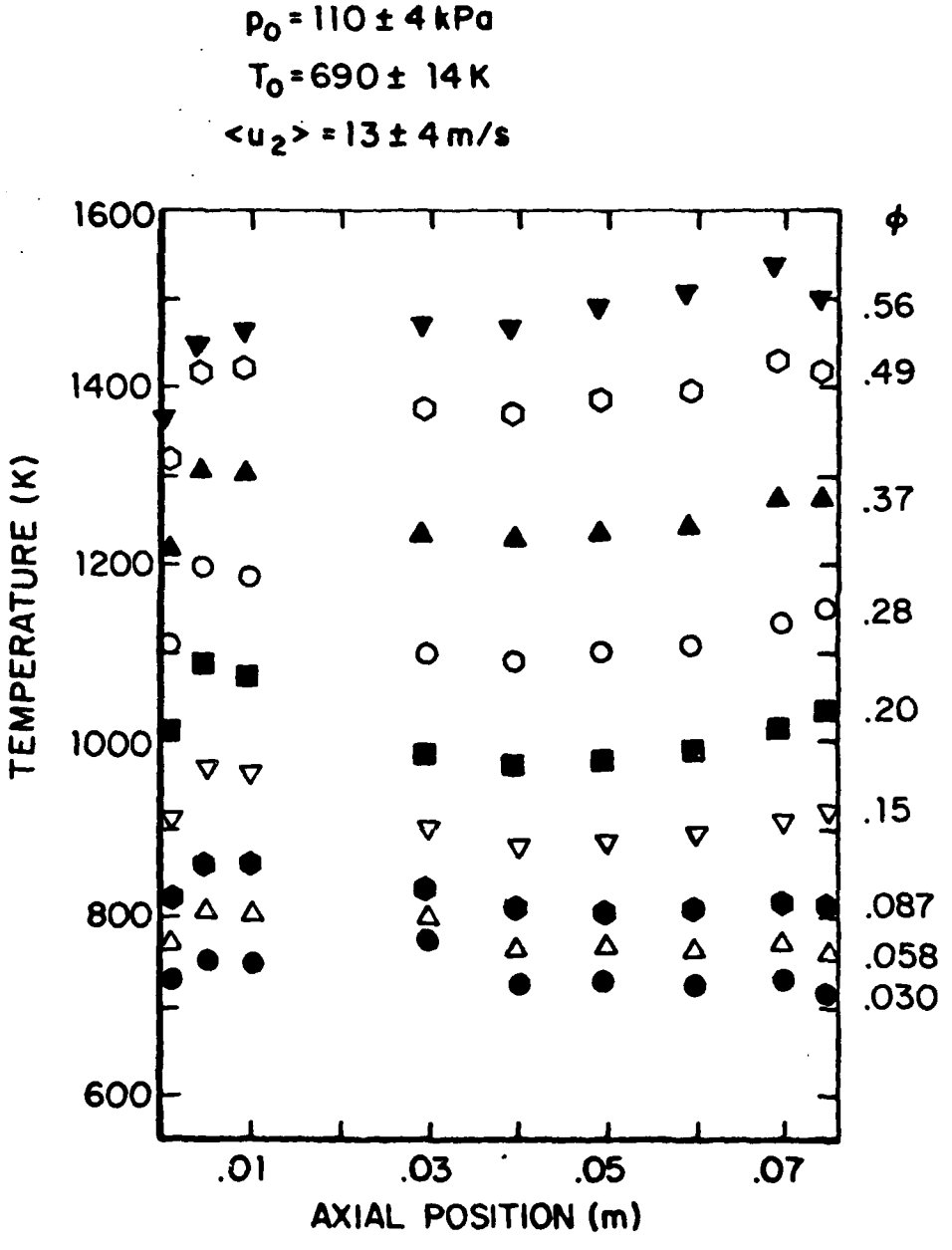

FIG. 15 SOLID TEMPERATURES $CO/O_2/CO_2$

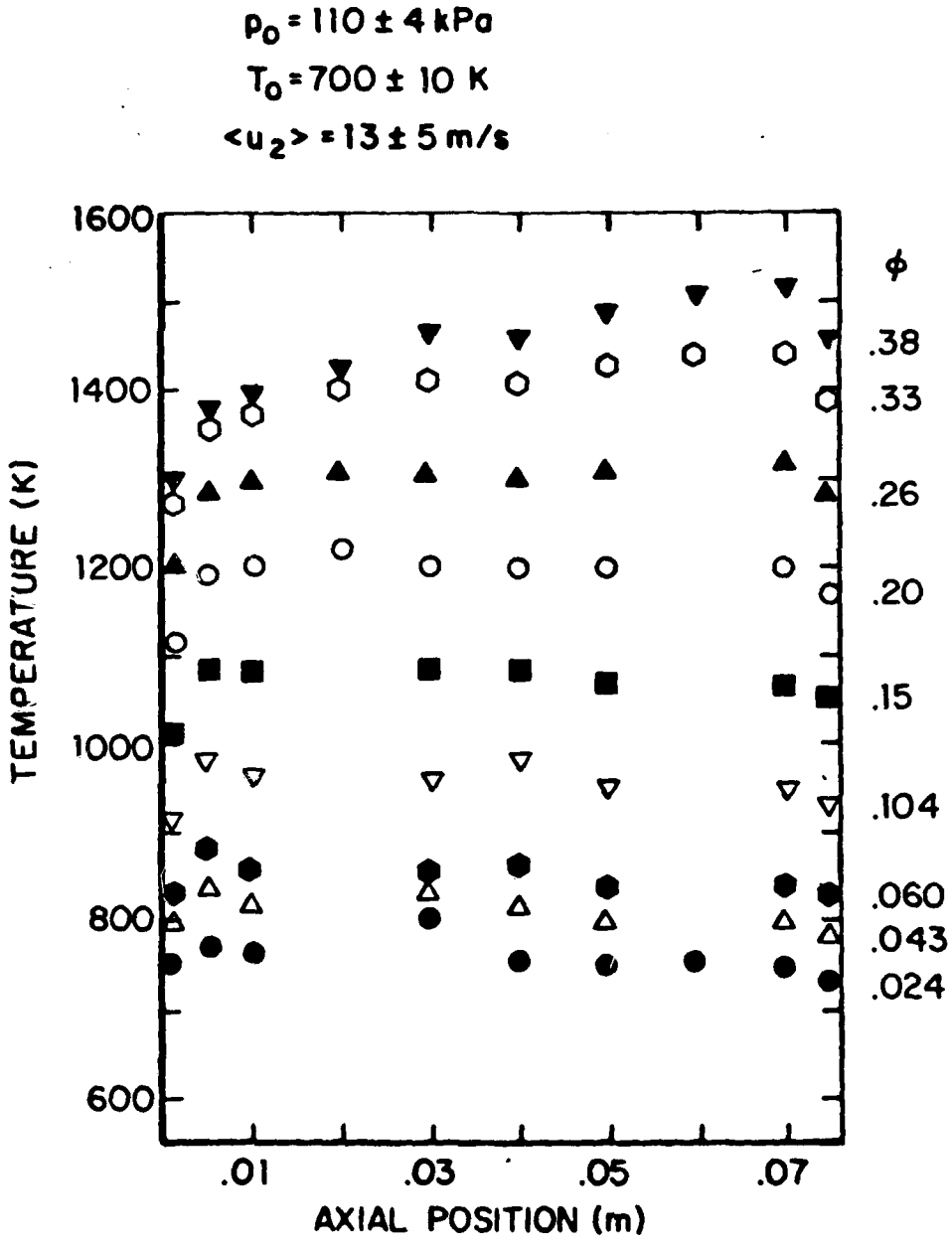

FIG. 16 SOLID TEMPERATURES $CO/O_2/N_2$

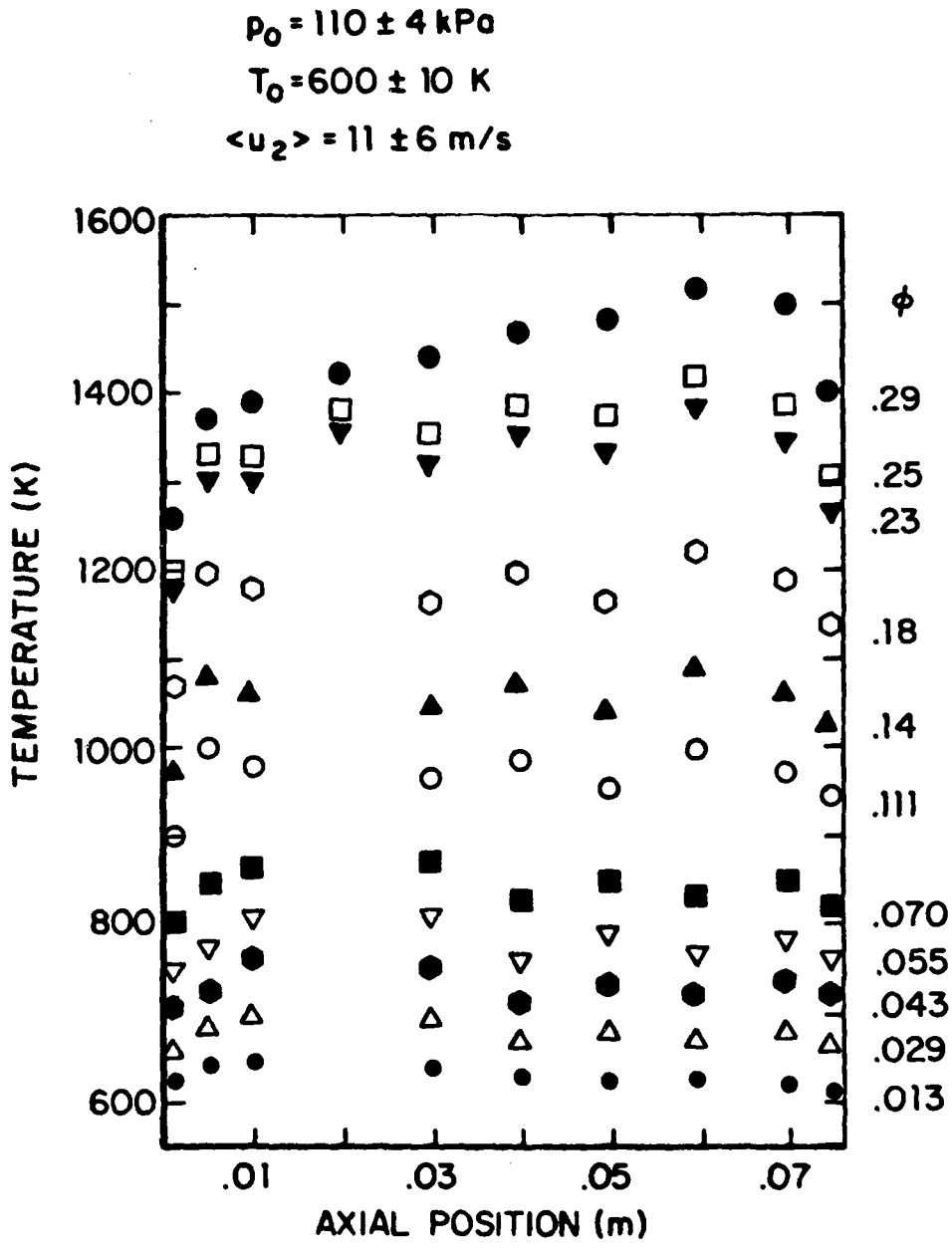

FIG. 17 SOLID TEMPERATURES: $CO/O_2/Ar$

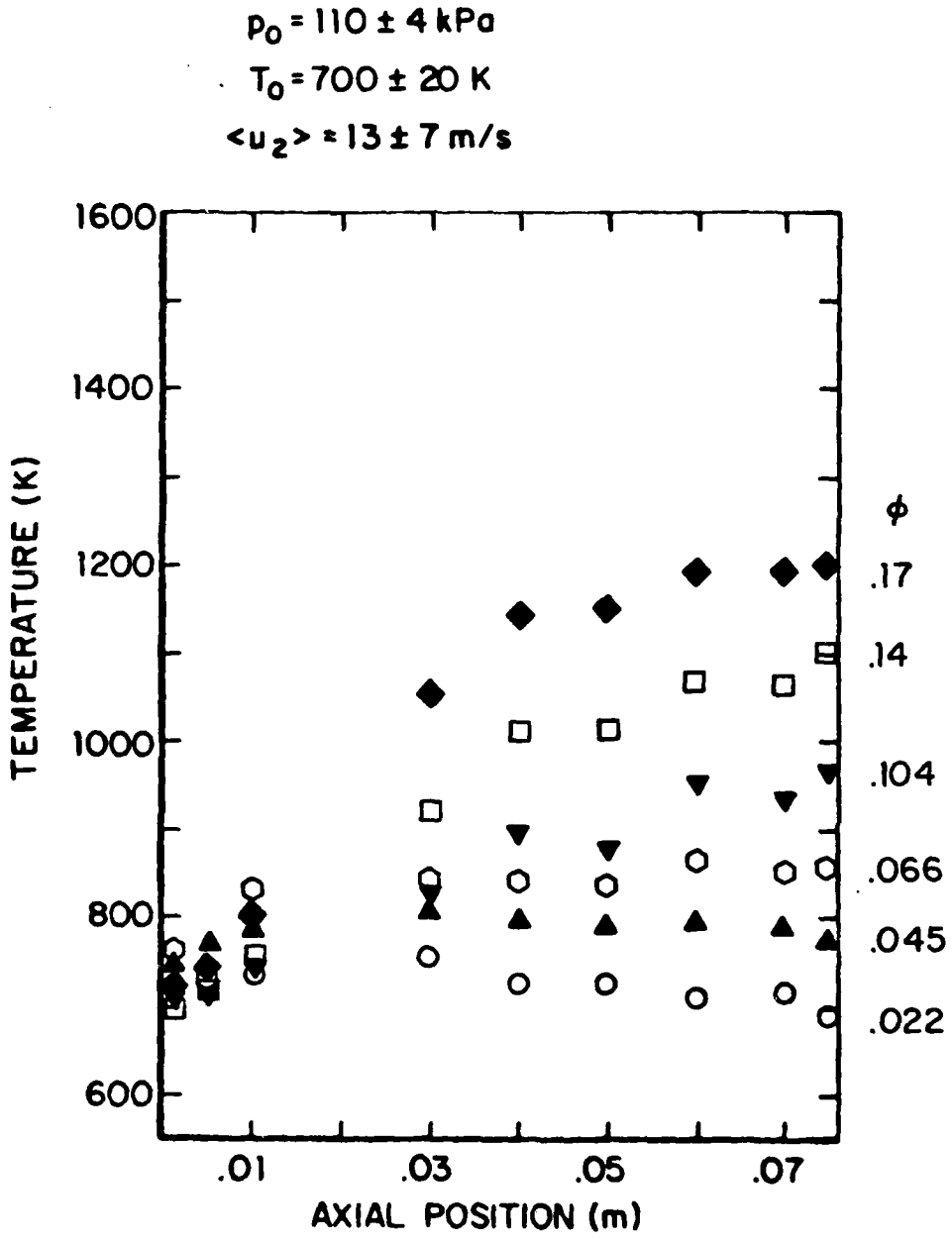

FIG. 18 SOLID TEMPERATURES $CO/O_2/He$

withstand the corresponding high temperature. These results again confirm the diffusion-controlled nature of the conversion process.

Two features of these experimental runs are immediately discernible when one compares the runs with N_2 as inert (Fig. 16) to the runs with air (Fig. 8) for the same equivalence ratios and velocities: 1. CO emissions are about 10 to 100 times higher and 2. they increase with ϕ rather than decreasing. Notice that emissions are higher for the $CO/N_2/O_2$ case even though the inlet temperature is 100K higher than for the CO/air case.

Degradation of the catalyst was at first suspected and then eliminated since the runs with $CO/N_2/O_2$ were performed immediately after the runs with CO/air. The only difference between the two series of runs is the water content of the inlet gas. In the CO/air runs the water molar fraction was 0.0054. In the runs with $CO/Inert/O_2$ the water content was determined by the H_2O present in the gas bottles, typically $\sim$0(1) ppm, and by the residual water left in the test rig by the preheating with air. No reliable measurements of H_2O were taken (due to the hygrometer characteristics) except for $CO/N_2/O_2$, where the H_2O molar fraction at the hygrometer station decreased during consecutive runs, i.e. as ϕ was increased, from 0.002 to 0.0004. It is conceivable that H_2O concentrations may have been even lower at locations further downstream of the hygrometer and close to the test sections. The gradual "flushing out" of H_2O during operation with dry mixtures parallels the abnormal emission trend with ϕ.

That CO oxidation depends on water content would not be surprising at all if took place in the gas phase. However, both experimental data and theoretical predictions indicate that almost all CO is converted to CO_2 at the catalyst surface and not in the gas, except for low velocity and high ϕ, where the gase phase contribution is (at most) 30% of the total CO converted. This, however, cannot explain the order(s) of magnitude

increase in the emissions. The only possible explanation must be that H_2O has a strong influence on the catalytic oxidation of CO on platinum.

This conclusion opens the door to some interesting speculations: it is known that gas phase oxidation of CO requires OH radicals (Gardiner and Olson, 1980). It is also known that platinum, and other Group VIII metals, tend to decompose H_2O and H_2O_2 through the tendency of Pt to chemisorb H atoms. It is therefore conceivable that at high temperature the conventional CO oxidation mechanism on Pt, proceeding via chemisorption of either or both CO and O_2 (Engel and Ertl , 1979; Campbell et al, 1980; Strozier, 1980) gives way to a different mechanism in which OH radicals produced at the platinum surface by the H_2O present in the incoming stream attack the CO molecules in a thin gas phase layer adjacent to the catalyst, thus actually simulating an heterogeneous oxidation. It is also interesting that high temperature OH desorption from Pt has been proposed as a "clean" source of OH for chemical kinetics studies (Talley et al, 1979; Talley et al, 1981). Low pressure studies indicate that OH escapes the surface only above a temperature $\sim 800^{\circ}K$ (Tevault, Talley and Lin, 1980). Even though catalytic processes generating radicals have been observed before and the term heterohomogeneous catalysis has been coined to describe them (Satterfield, 1980), this is the first time that they are reported as possibly present in a practical combustion device. Further work is in progress to check quantitatively the oxidation mechanism postulated above.

c) C_3H_8/Air Mixtures

Some of the theoretical results are shown in Figs. 19 through 30. Figure 19 shows the monotonical decrease in HC concentration along the axis and from the axis to the catalytic wall. The rate of HC breakdown and oxidation is a function of the radial mass transfer and of the CO oxidation rate. Increasing

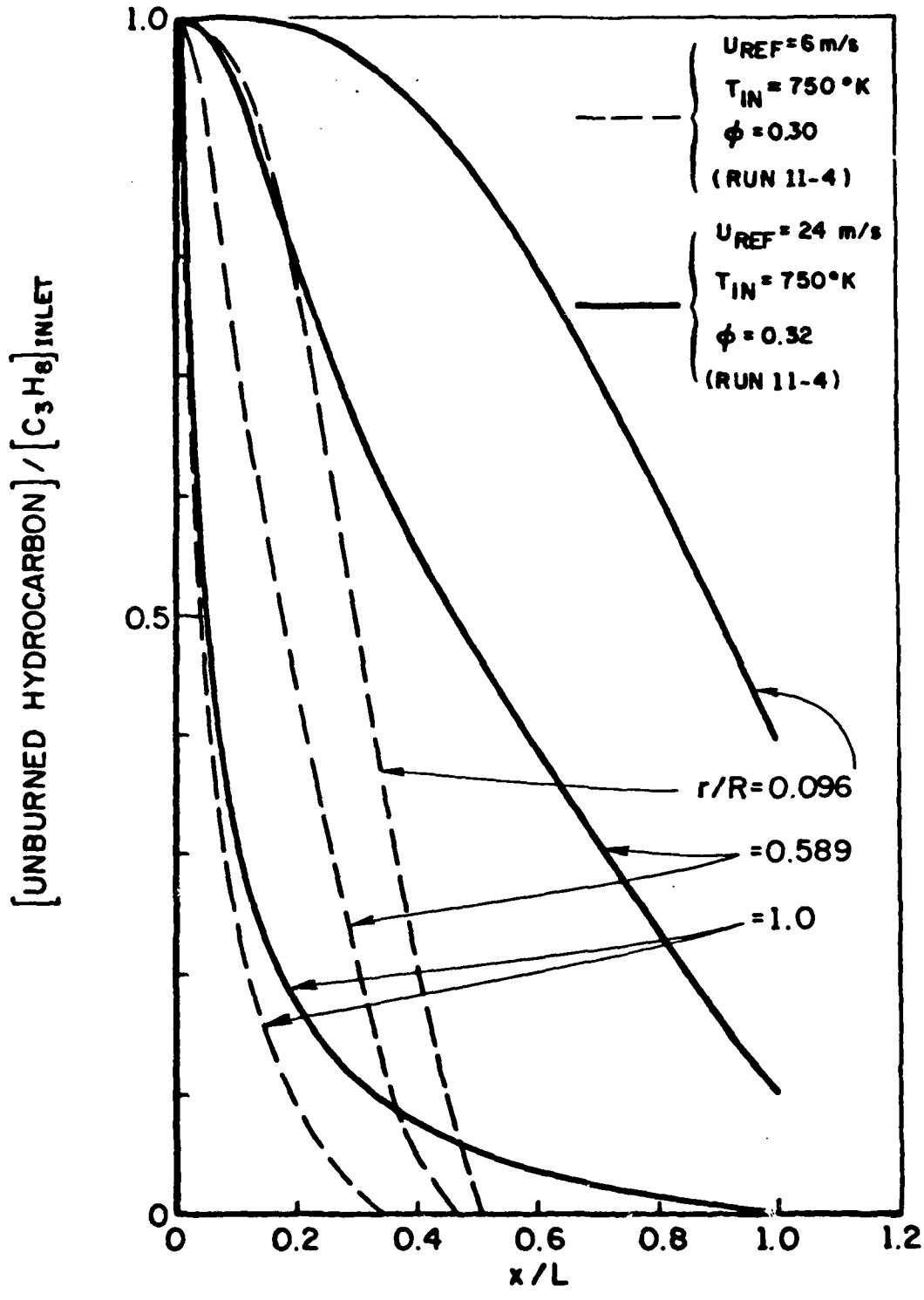

FIG. 19. UHC Axial Concentration Profiles - Effect of Velocity

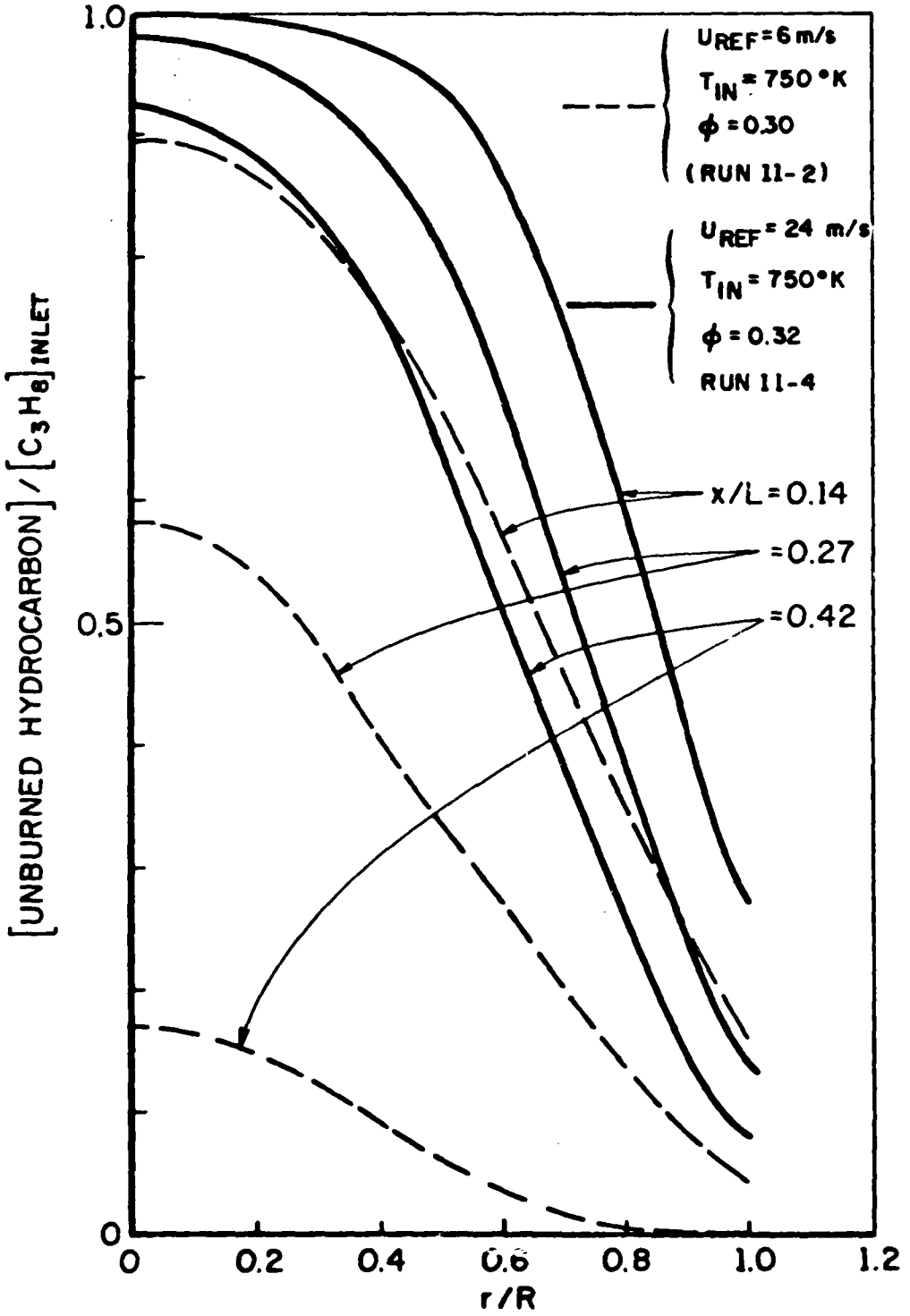

FIG. 20. UHC Radial Concentration Profiles - Effect of Velocity

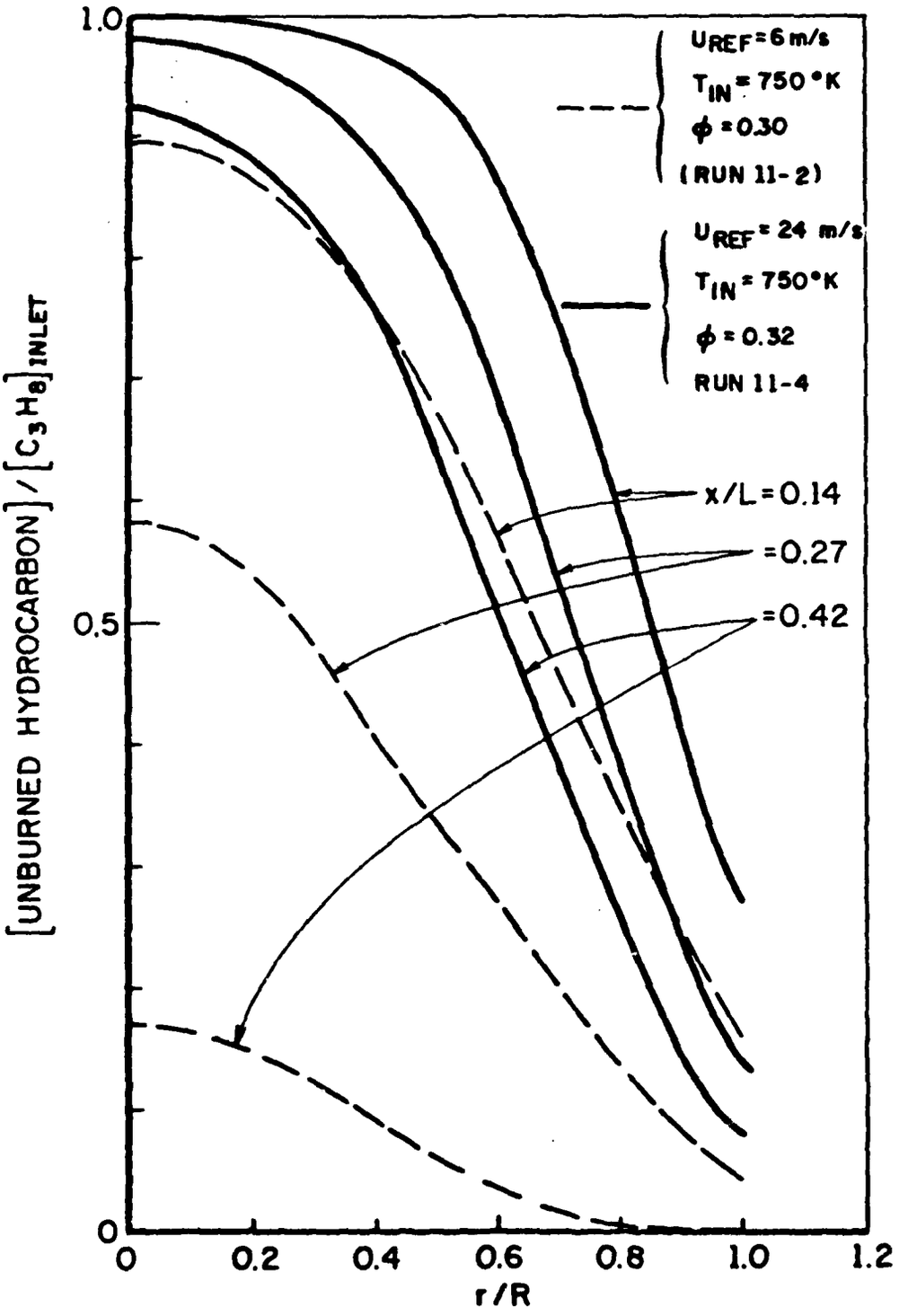

FIG. 20. UHC Radial Concentration Profiles - Effect of Velocity

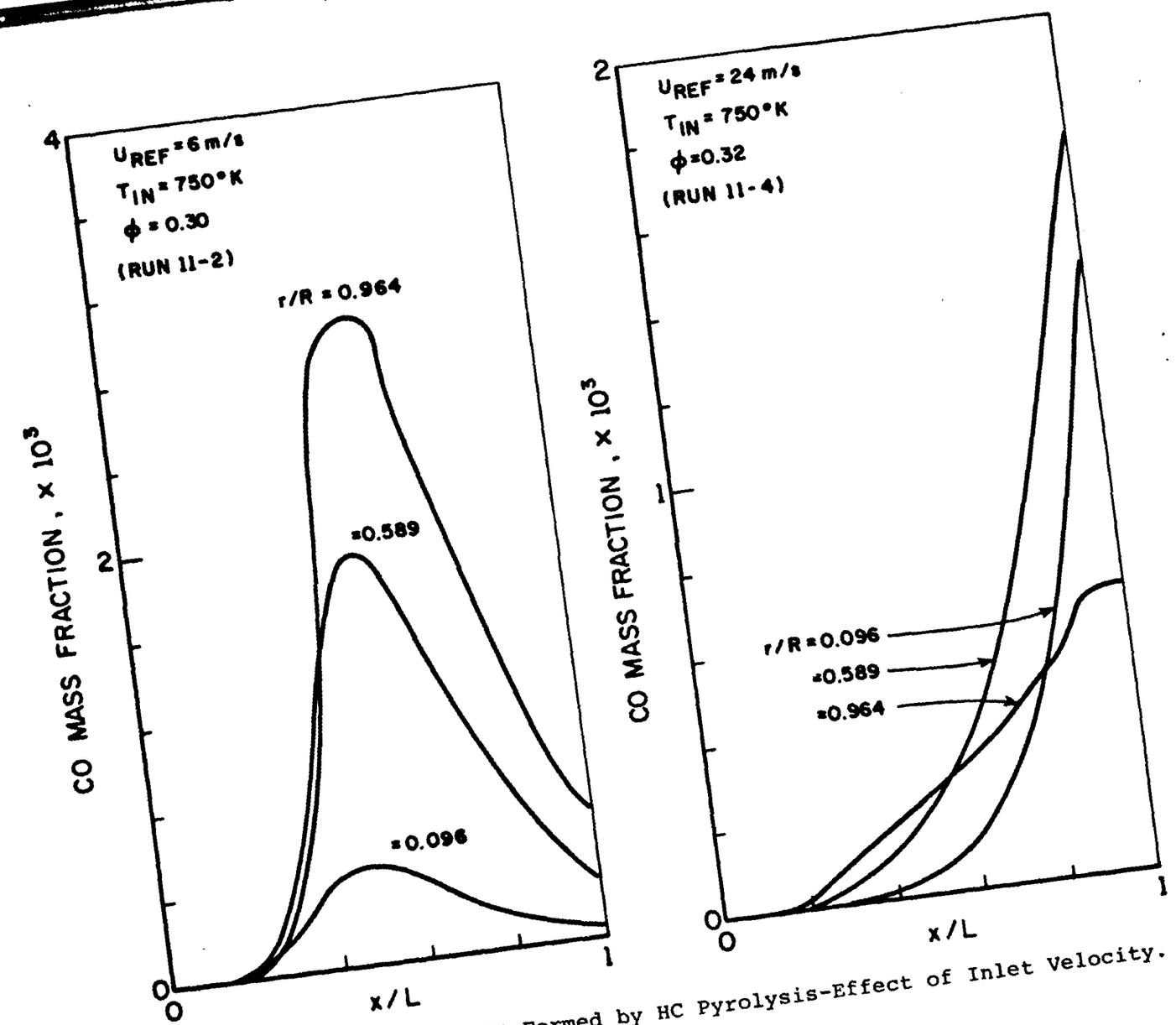

FIG. 21. Axial Profiles of CO Formed by HC Pyrolysis-Effect of Inlet Velocity.

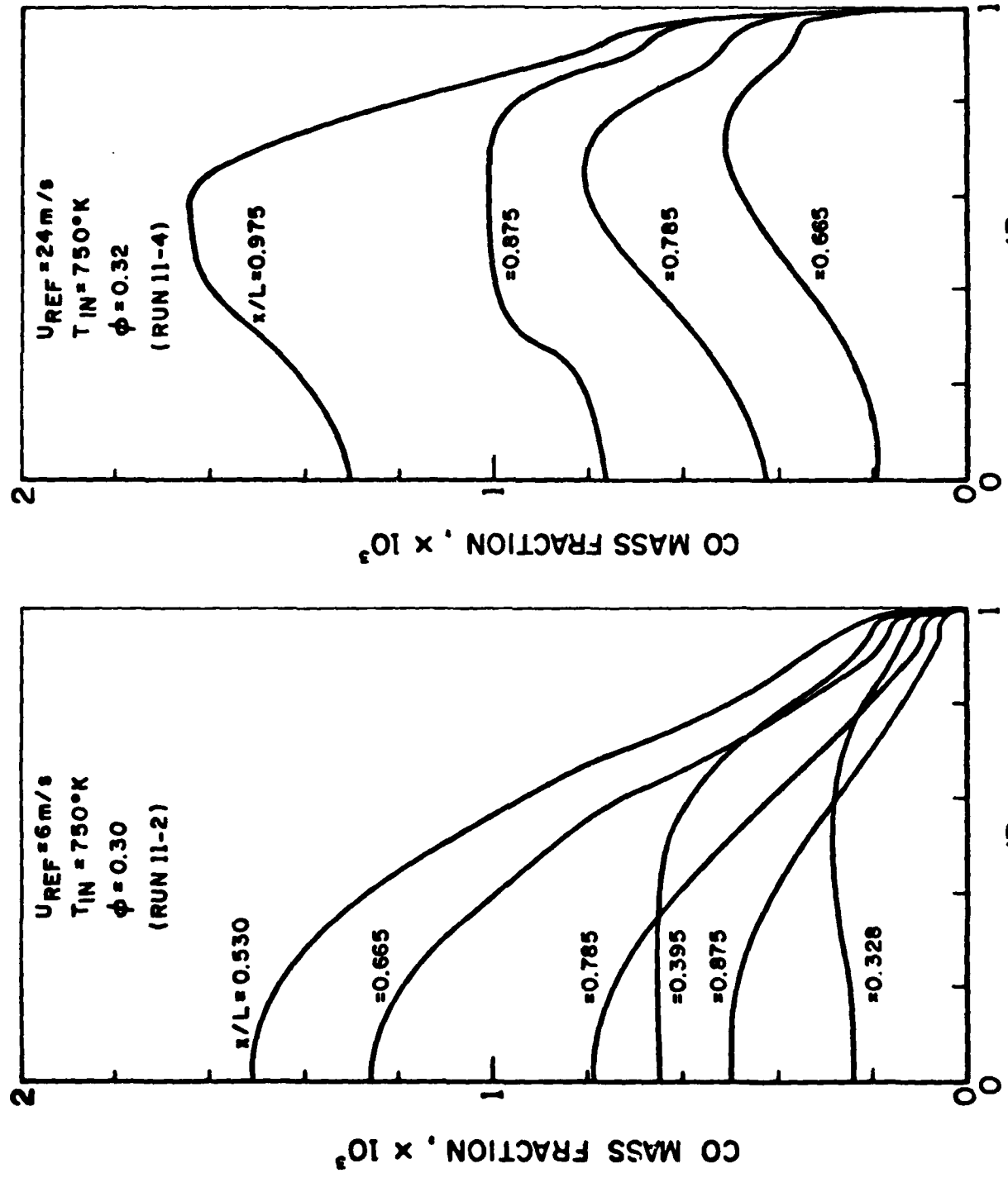

FIG. 22. Radial Profiles of CO Formed by HC Pyrolysis-Effect of Inlet Velocity.

the inlet velocity, as in Fig. 20, results in a correspondent decrease in residence time and a slower HC disappearance.

The large gradients at the wall and throughout most of the channel cross-section indicate that the two-dimensional modeling of the fuel conversion is necessary for its adequate description.

CO formation and destruction is shown in Figs. 21 and 22 for the same two cases of low and high inlet velocity. At u_{ref} = 6 m/s the residence time is sufficiently large for CO to form and be oxidized mostly within the channel length. The radial CO profiles of Fig. 22 indicate an initial bulge, or maximum, for r/R $\sim$ 0.6 near the inlet, where gas phase production of CO becomes larger than its consumption both in the gas phase and at the wall. Further inside the channel propane and ethene pyrolysis keep producing more and more CO; a peak appears in fact at approximately x/L = 0.5. Past the channel half-length the high temperature speeds up the gas phase rate of the CO $\rightarrow$ CO_2 reaction, and CO decreases rapidly. Local changes in the radial profiles slopes reflect the interplay of the three mechanisms at work for CO - production and consumption by gas phase pyrolysis, and consumption at the wall. Generally speaking, near the wall the rate of formation is high because of the high temperature; however diffusion is also fast and CO consumption is high. Therefore near the wall CO concentration is generally low and is accompanied by sharp gradients.

Away from the wall instead, the dominant effects are CO formation by C_3H_8 and C_2H_4 pyrolysis, and oxidation to CO_2 in the gas. Local bulges indicate CO accumulation, i.e. that the first phenomenon is quantitatively more important than the second; however, contrary to what happens near the wall, CO levels may be high, since gas phase CO oxidation is not as fast as diffusion transport near the wall.

At the higher velocity (u_{ref} = 24 m/s, see Fig. 21) there is no time for CO to be oxidized appreciably within the channel,

and axial profiles are monotonic, showing that a CO peak would presumably occur downstream of the outlet.

Overall comparison between theory and experiments is shown in Figs. 23 through 30. The pressure drop between catalyst inlet and outlet is important for gas turbine applications. There is a certain amount of disagreement between predictions and data; this is likely to be the effect of having approximated the (roughly) trapezoidal shape of the channel cross-section by a circular one. The trends, however, are reproduced (see Fig. 23). Figure 24 shows good agreement in the UHC emissions comparison.

All the trends are reproduced and do not present particular problems of interpretation. Less quantitatively satisfactory are the predictions of the CO outlet emissions, although the trends are again correctly predicted. The increase of CO with ϕ and inlet temperature is due to the faster rate of C_3H_8 and C_2H_4 pyrolysis forming CO more rapidly inside the monolith and eventually reducing CO emissions. The same result could of course be obtained by increasing the residence time, i.e. the monolith length. The range of velocities investigated did in fact reveal the same residence time effect: the highest velocity has effect similar to the lowest ϕ and T_{in}, and when velocity is sufficiently low the emission decrease after reaching a maximum. This maximum therefore occurs when the cross-section averaged rate of CO production is balanced by gas-phase and surface consumption right at the monolith exit. Since these rates depend on kinetics, at each velocity there will be a ϕ and an inlet temperature for which CO emissions will peak. Conversely, for fixed kinetics (fixed ϕ and T_{in}) there will be a velocity for which CO emissions will peak.

Reasonably satisfactory in a quantitative sense are also CO_2 and O_2 predictions (Figs. 26 and 27). The CO_2 trend is opposite to the trends of UHC and O_2, since CO_2 is a final product of HC oxidation.

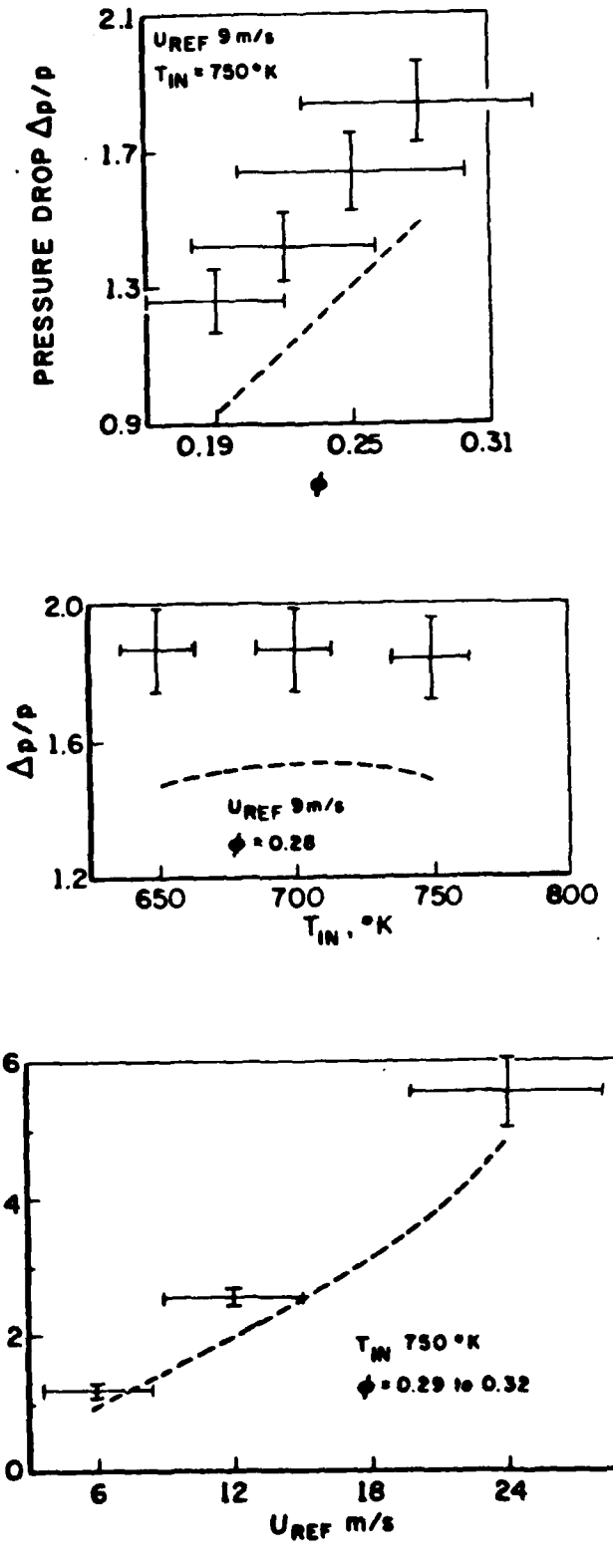

FIG. 23. % Pressure Drop in a Monolith Channel as a Function of ϕ, Inlet Temperature and Velocity. C_3H_8/Air Oxidation on Pt.

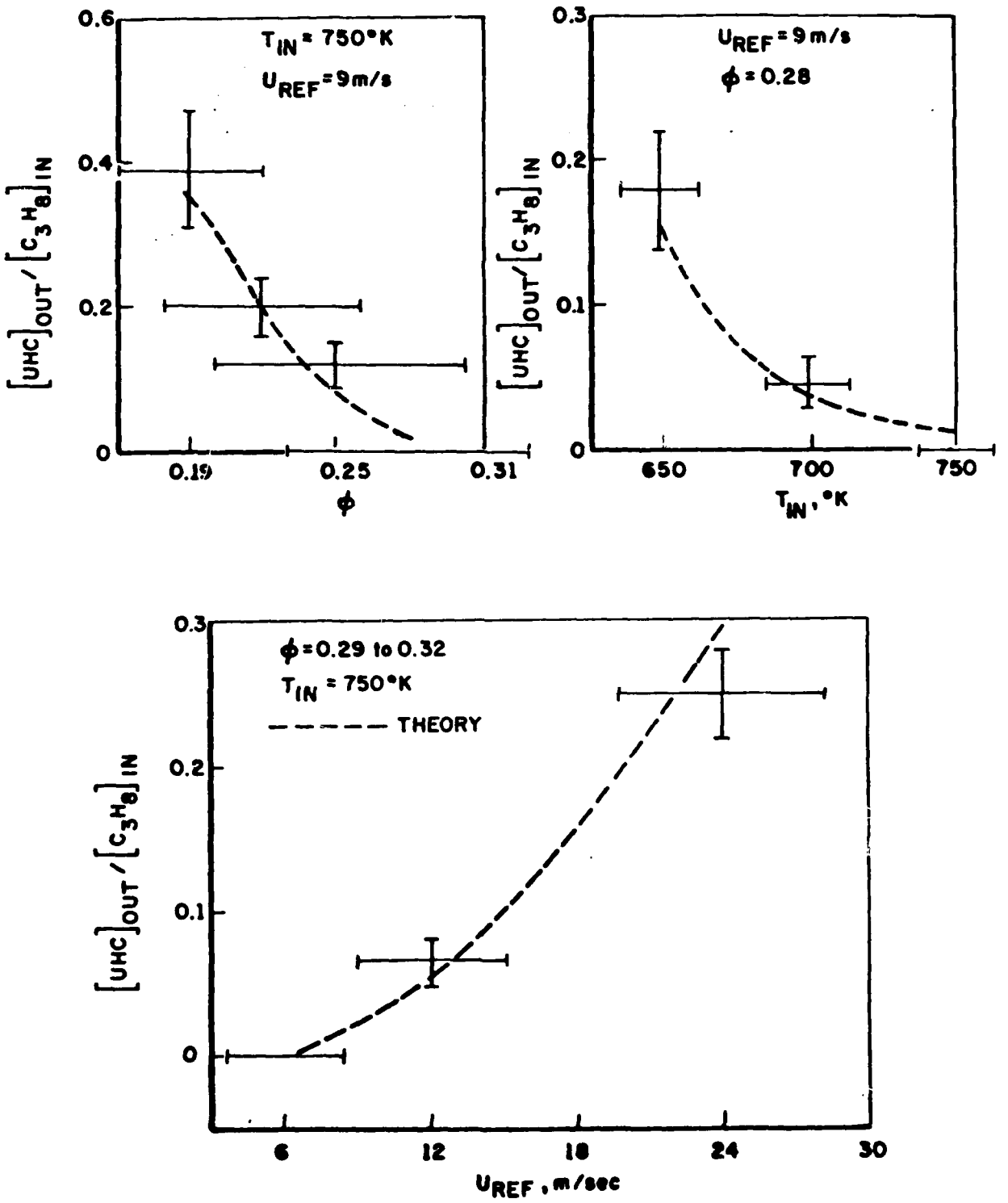

FIG. 24. Outlet/Inlet UHC Emission Ratio for C_3H_8/Air Oxidation on Pt - Effect of ϕ, Inlet Temperature and Velocity

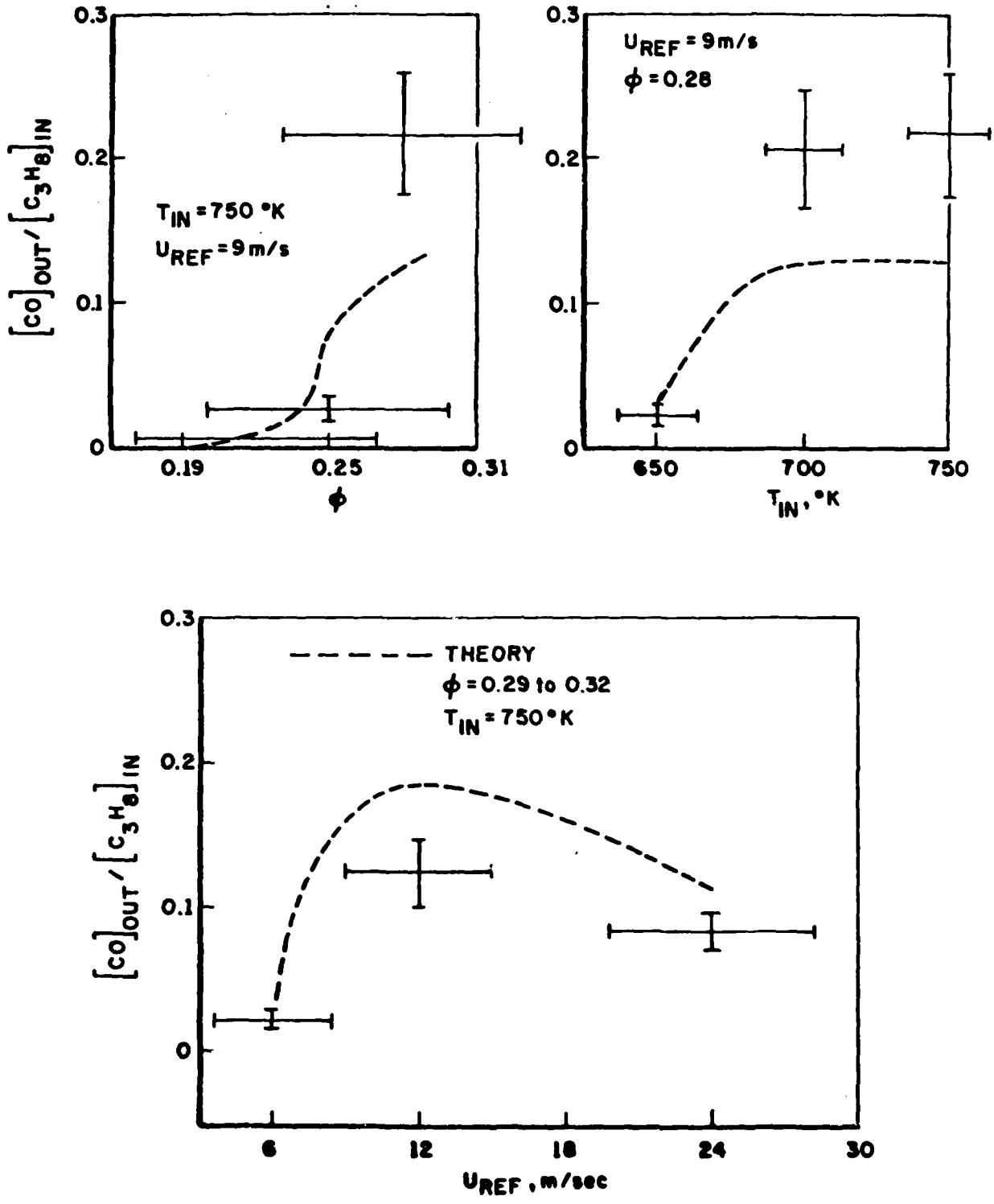

FIG. 25. CO Outlet Emissions for C_3H_8/Air Oxidation on Pt - Effect of ϕ, Inlet Temperature and Velocity

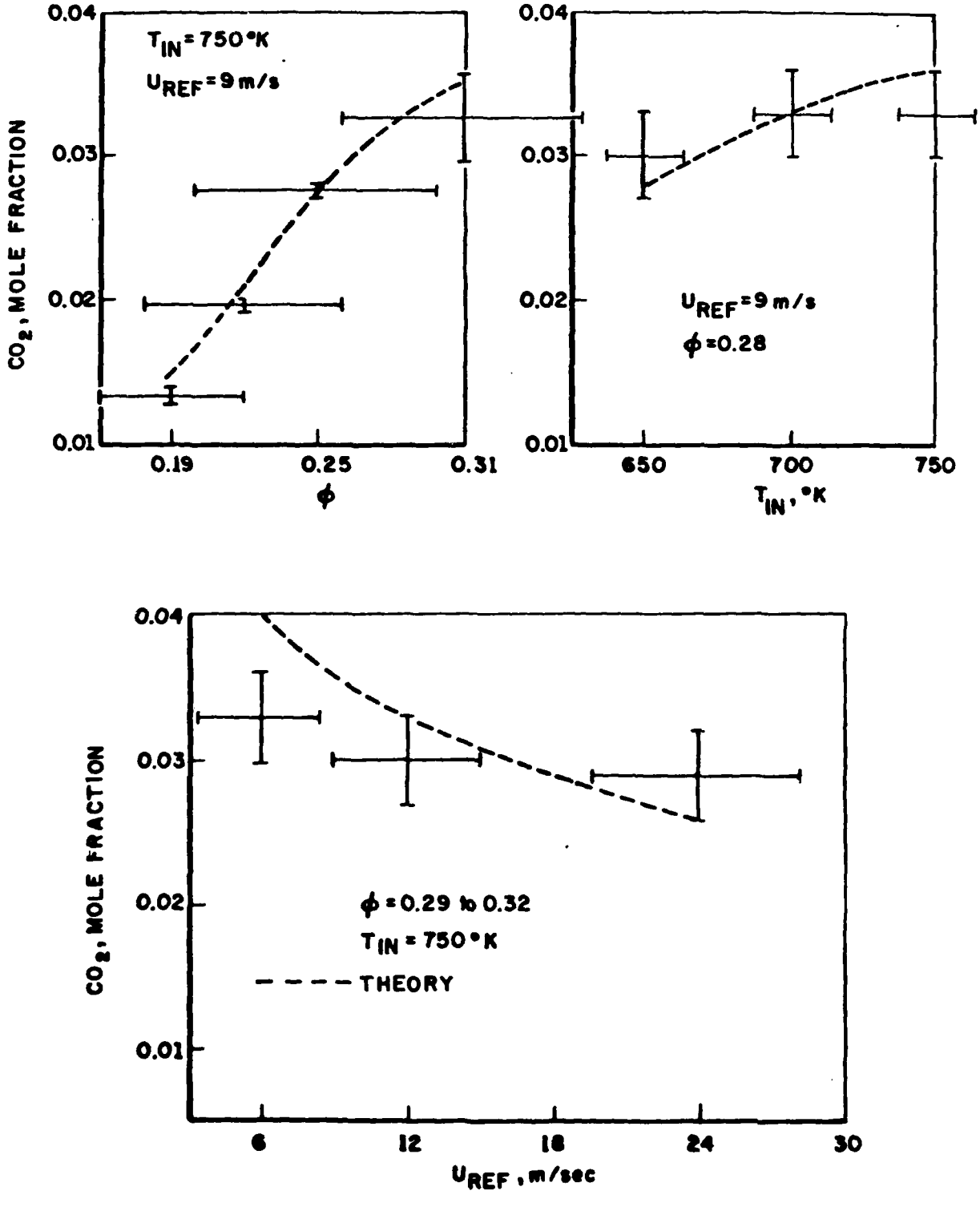

FIG. 26. CO_2 Outlet Emissions for C_3H_8/Air Oxidation on Pt - Effect of ϕ, Inlet Temperature and Velocity

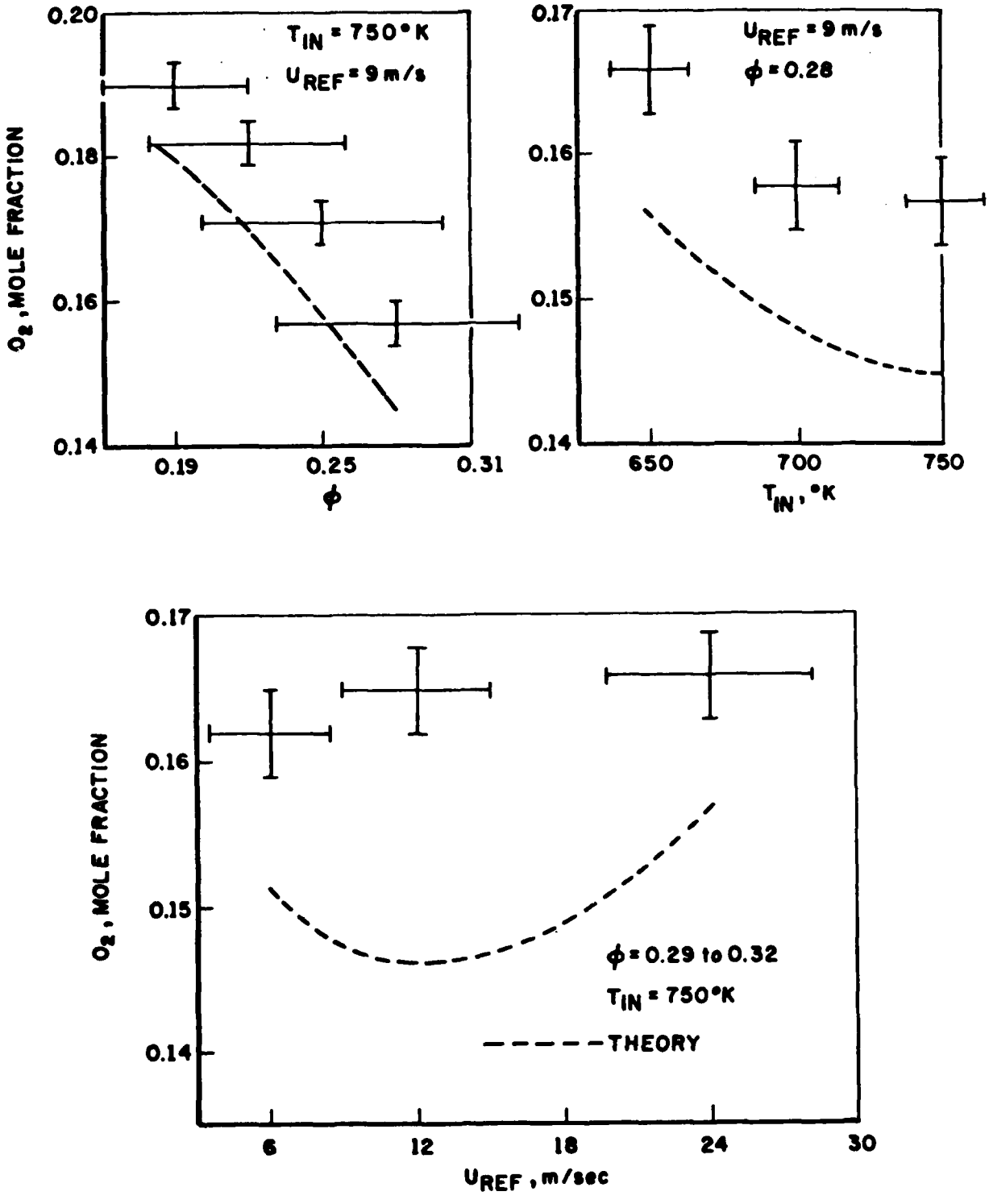

FIG. 27. O_2 Outlet Emissions for C_3H_8/Air Oxidation on Pt - Effect of ϕ, Inlet Temperature and Velocity

Since the agreement between measured and predicted quantities is reasonable, the mathematical model may be trusted to derive some interesting conclusions concerning the relative importance of the many physico-chemical phenomena that take place inside a monolith channel.

The effect of diffusion was tested by varying the temperature-dependent fit of the C_3H_8 diffusion coefficient. Information on C_3H_8 diffusion is sketchy at the temperatures of interest in the present work (Lannus, 1970; Barr and Watts, 1972; the exponent n for the C_3H_8 fit

$$D_{C_3H_8/Air} = D_o \left(\frac{T}{T_o}\right)^n$$

was chosen on the basis of the good agreement with the experimental data and of the theoretical information available. In doing so the effect of diffusion became readily apparent: propane emissions changed by almost one order of magnitude when n was changed from 1.74 to 1.95. Diffusion therefore has a large effect on propane conversion. However a case for the process to be diffusion-controlled may not be made, since the propane heterogeneous rate is finite. In fact, no reasonable results could be obtained when the wall reaction was assumed infinitely fast (i.e. diffusion was assumed controlling). A further look at Figs. 28 through 30 illustrates the situation. In all three the ratio

$$r_{GS} \equiv \frac{\int_V \dot{\omega}_k \, dV}{\int_A \dot{\omega}_{Wk} \, dA} \qquad (k = C_3H_8,\ C_2H_4,\ CO)$$

is plotted as a function of the inlet parameters. The term upstairs is the overall rate of conversion of fuel species k due to homogeneous reactions in the gas, while the term downstairs expresses the corresponding catalytic rate of conversion at the wall.

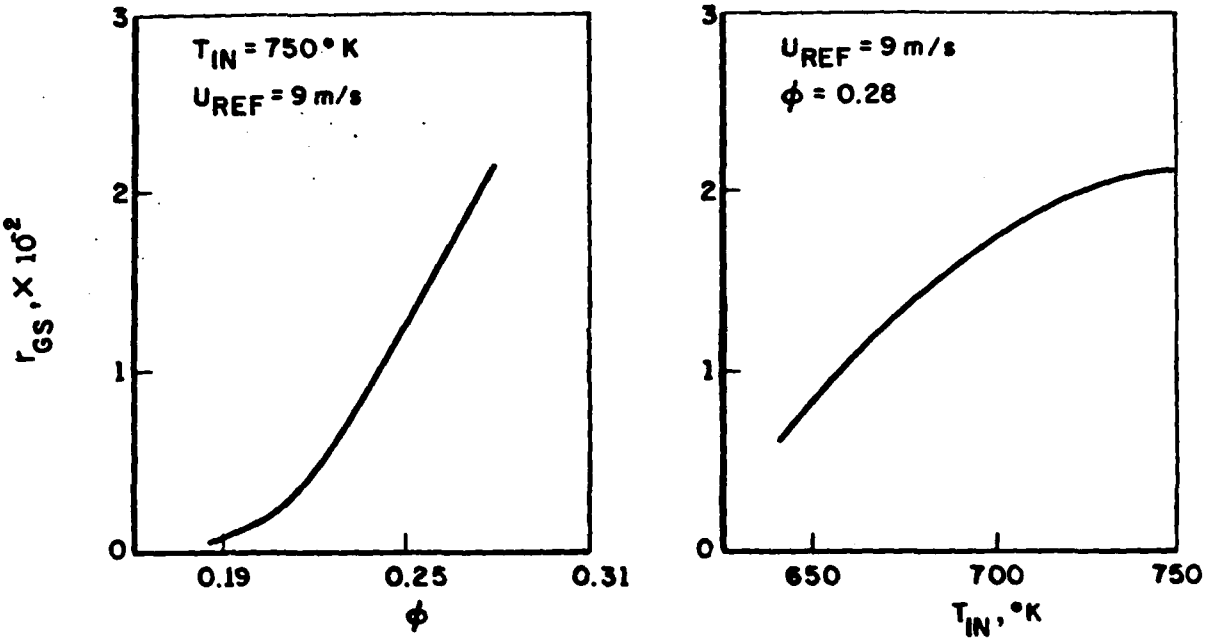

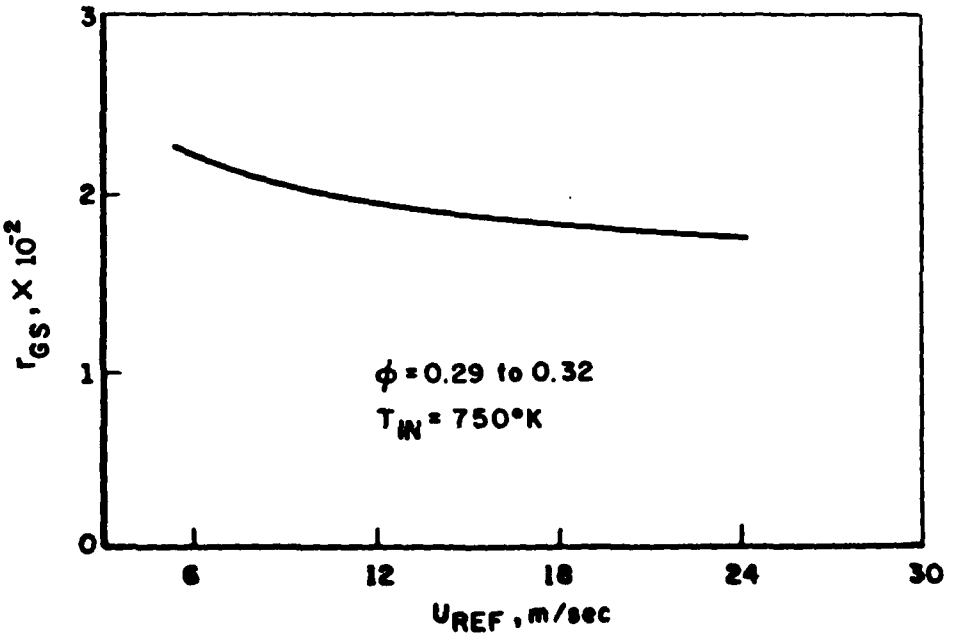

FIG. 28. Gas Phase/Surface C_3H_8 Consumption Ratio r_{GS} for C_3H_8/Air on Pt. - Effect of Inlet Parameters

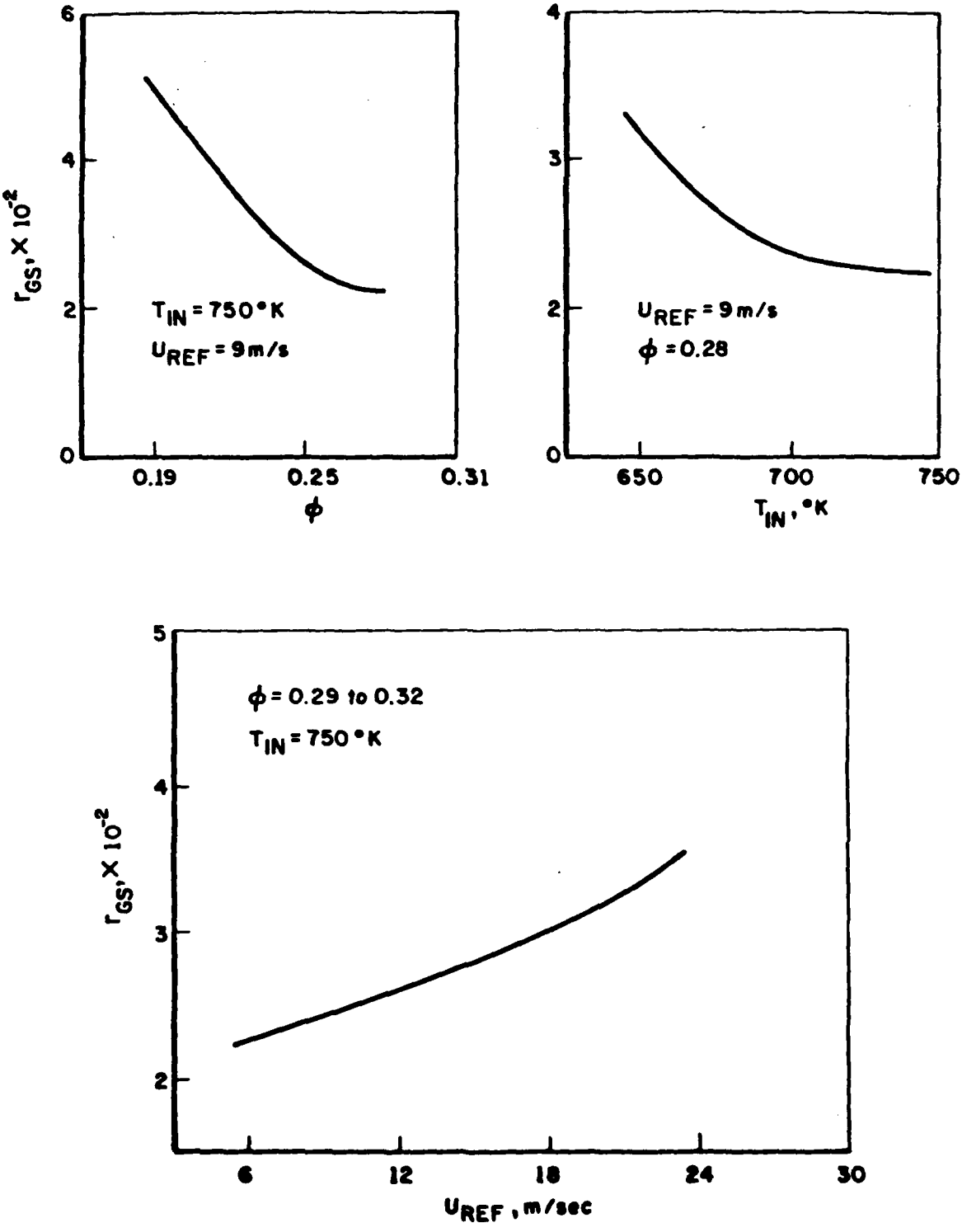

FIG. 29. Gas Phase/Surface C_2H_4 Consumption Ratio r_{GS} for C_3H_8/Air Platinum - Effect of Inlet Parameters

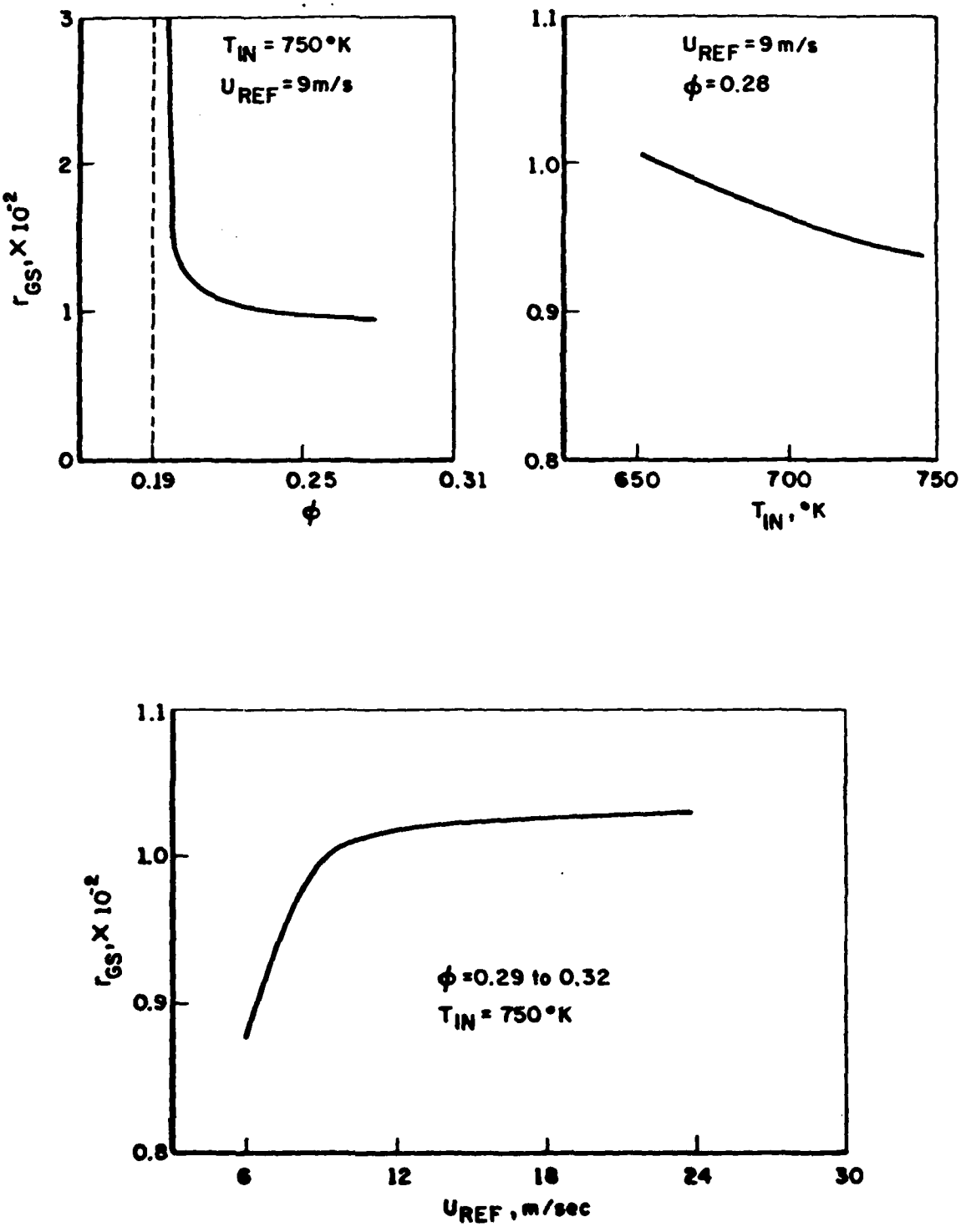

FIG. 30. Gas Phase/Surface CO Consumption Ratio r_{GS} for C_3H_8/Air Over Platinum - Effect of Inlet Parameters

For propane (Fig. 28) r_{GS} increases with ϕ and T_{in}, i.e. with chemical kinetics. This means that the homogeneous conversion becomes more and more important than heterogeneous conversion. The effect of ϕ and T_{in} is felt both by $\dot{\omega}_k$ and $\dot{\omega}_{wk}$; however the Lewis-Semenov number for C_3H_8 in air, i.e.

$$Le = \frac{K}{C_p \rho D_{C_3H_8/Air}}$$

varies between 1.5 and 1.3 between 900 and 1200°K, i.e. in the range of temperatures of interest in this study. Thus the effect of raising heterogeneous kinetics is more than compensated by the larger heat feedback from the wall into the gas, with its corresponding effect on homogeneous conversion. This one tends to decrease with reduced residence times, while heterogeneous conversion is practically independent on velocity, since the wall temperature depends practically on ϕ and T_{in} only. This explains the r_{GS} trend with increasing reference velocity. Far more interesting is the actual magnitude of r_{GS}, showing that gas phase dominates over surface in converting propane (and C_2H_4 and CO as well). This result should not be interpreted as meaning that the catalytic surface has no effect on C_3H_8 conversion. In fact C_3H_8 pyrolysis times at the inlet temperatures of this study are exceedingly long, i.e. of the order of 10^1 seconds, while residence times are $\sim 10^{-3}$ seconds. No measurable propane conversion can take place within a monolith of the length used without a catalyst. The effect of platinum is therefore to release heat that feeds back into the gas at a rate faster than the rate at which propane may diffuse to the wall to react (i.e. Le > 1). Under these conditions, and for the channel size used, the gas is where most of the fuel is converted. In the catalytic oxidation of CO in air (see section C.a) the opposite result holds true; the two situations differ in that propane reacts at the wall at a finite rate rather than infinitely fast, its diffusion coefficient is less than half of the CO coefficient at the same temperatures, and the

Lewis number is larger than one.

The trends observed in Fig. 28 are reversed in the case of the two other fuel species (see Figs. 29 and 30). Both species are formed by previous reactions and are not initially present in the channel. Their formation takes place where the temperature is higher, i.e. near the wall, which is also where they can diffuse faster to react on the catalyst. Therefore an increase in the kinetics parameters (ϕ and T_{in}) raises the temperature preferentially near the wall. The characteristic times for C_2H_4 and CO homogeneous breakdown become smaller at a rate slower than diffusion times to the wall.

The effect of velocity tends to oppose ϕ and T_{in}. The longer the residence time the higher the amount of formed species that may diffuse to the wall and be oxidized there. Therefore it is to be expected that raising the flow velocity tends to increase the importance of gas phase conversion of C_2H_4 and CO.

From this discussion it is apparent that no dominant elementary mechanism may be invoked to characterize propane oxidation in air in the range of parameters explored.

D. NEW CATALYST

The importance of the solid phase in the oxidation of C_3H_8 and CO has pointed out the necessity of investigating in a more detailed physical way the nature of the catalytic material. This requires an understanding of the bulk and surface properties of the catalyst and their temperature dependence as well as the establishment of criteria that take into account chemistry and physics at the lattice level and relate these phenomena to the global catalytic combustion reaction.

The platinum-coated cordierite used so far does not lend itself to an easy characterization, due to a lack of knowledge of the uniformity and thickness of the coating, of the interaction between the γ-alumina washcoat and the substrate during

operation, and of the aging process when platinum is lost due to its high volatility. In addition, the cordierite cannot sustain temperatures higher than 1473^{o}K and this represents an undesirable barrier from the thermodynamic viewpoint.

In light of the difficulties inherent in the coated substrates mentioned above, efforts have gone into the design of a monolithic single-phase catalytic material with a low light off temperature and an improved high temperature stability.

Initial considerations of the nature of the catalytic process in which a gas phase molecule is adsorbed and undergoes reaction followed by desorption of product(s), leaving the adsorption site free for subsequent iterations, indicate that the surface sites must be capable of (reversible) changes in valence state. This is most readily assured by making the material an electronic conductor. A substantial body of research has been performed in the investigation of high temperature conductive materials for use as MHD electrodes, and the most promising candidates for that application are perovskite ceramics. Perovskites, of general formula ABO_3, have a cubic (or near-cubic) lattice in which the B sites occupy the corners of the unit cell, an A site is in the cell center, and the oxygen atoms are at the edge centers. Typical MHD materials that have good erosion resistance at high temperatures as well as room temperature resistivities in the range 1-10 Ωcm are modifications of the perovskite compounds $LaAlO_3$, $MgCrO_3$, etc. It is possible to introduce the necessary properties for enhanced catalytic activity while still preserving high temperature stability, electronic conductivity and low erosion rate by suitable modification of the A and B sub-lattice constituents (See Fig. 31).

Introduction of a strontium dopant on the A sites in the material $La_{.94}Sr_{.16}CrO_3$ produces a p-type material having decreased electrical resistivity as well as increased volatility (Meadowcraft, 1969) (See Fig. 32). To reduce the volatility, aluminum can be introduced into the B sites, as in $LaAl_{.5}Cr_{.5}O_3$,

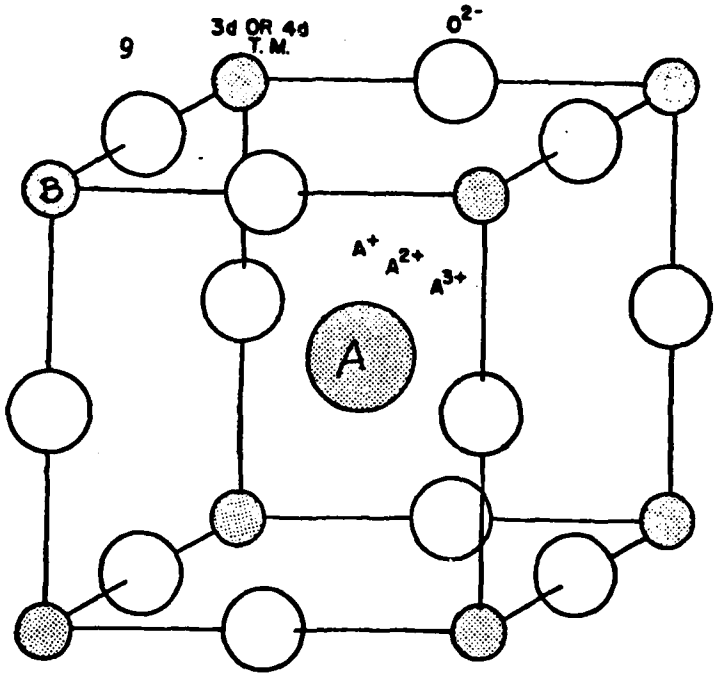

Fig. 31. Perovskite Crystal Structure (from Voorhoeve et al., 1976)

which is extremely stable at high temperatures. Mass loss measurements on this material show that the mass loss rate declines with increasing Al content up to atomic fraction 0.5 of the B sites, after which the loss rate remains essentially constant; the aluminum serves to stabilize the chromium in the lattice, which otherwise volatilizes as chromium oxides (Anderson, 1978) (Fig. 33).

Catalytic behavior of mixed perovskite materials shows moderate activity for CO oxidation but high light-off temperatures and susceptibility to poisoning by SO_2. Addition of platinum in quantities >1600 ppm to the materials $La_{.7}Pb_{.3}MnO_3$ and $La_{.7}Sr_{.3}MnO_3$ resulted in a lowered light-off temperature and performance comparable to commercial supported Pt catalysts (Voorhoeve, 1976).

Motivated by the general influences outlined above of material composition on performance characteristics, we have chosen the material $La[Mg_{.6-x}Pt_xCr_{.47}Al_{.47}]O_3$, with $.001 \leq x \leq .01$, as our monolithic combustion catalyst. We estimate this material will exhibit catalytic activity comparable to that of platinum coated substrates, remain as a single phase over a wide temperature range, and have suitable low light-off temperatures. The platinum is chemically bound into the material rather than present as islands of free metal, and can therefore be expected to have low volatility. The magnesium will exist in the lattice as Mg^{2+} which will serve to charge-compensate the Pt^{4+} and make its incorporation into the lattice more probable.

A sample of this material, with x = .01, has been prepared for us (by Prof. H.U. Anderson, University of Missouri/Rolla), and an x-ray diffraction analysis (by Dr. G.J.B. Williams and Mr. J. Hurst, Brookhaven National Laboratory) of the powder indicates that the material is approximately cubic and consists of a uniform single phase, with lattice parameter 3.855 Å, in the range expected for perovskites. Atomic adsorption measurements performed at Princeton have indicated the presence of the

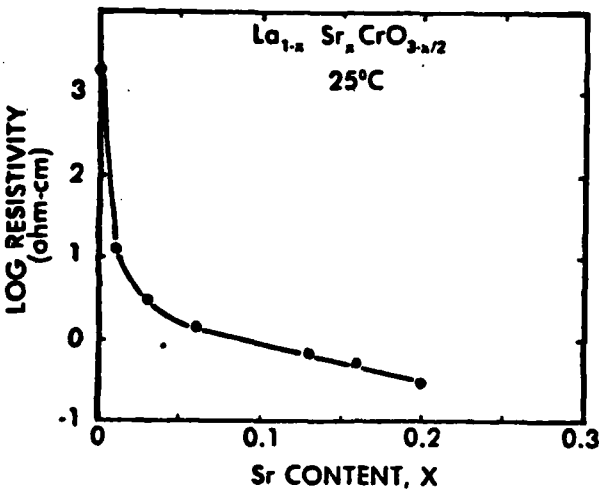

FIG. 32 (from Meadowcraft, 1969)

Electrical Resistivity of $La_{1-x}Sr_xCrO_3$ as function of Sr content

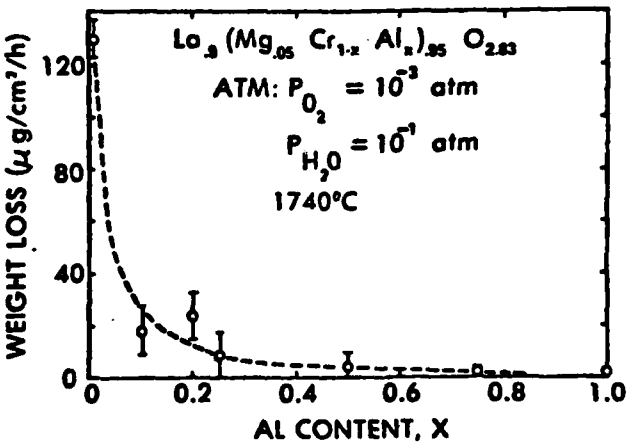

FIG. 33 (from Anderson, 1978)

Weight loss (Mg/cm²/h) of $La_{.9}(Mg_{.05}Cr_{1-X}Al)_{.95}O_{2.83}$ as function of Al content: Temperature = 1740°C; Atm: Flowing gas mixture (0.001 atm O_2+0.1 atm H_2O+N_2); Flow rate = 1 linear cm/sec.

expected amount of platinum; however, since this quantity is small it is still possible that it is present in a second phase which is not detectable by the x-ray measurements.

Our design for the catalyst unit geometrical configuration is expected to prove practicable for actual combustion applications, relatively easy to fabricate and have well-defined flow channels amenable to exact flow modeling calculations. The latter criterion is essential for model development but will not be a constraint on actual combustor design. The catalyst configuration will consist of a stack of flat plates separated by spacers at their edges, creating high aspect ratio channels between the plates. The plate dimensions will be approximately 2" x 5" x .050", and the spacing will be variable from .050" to ∿0.2". These dimensions have been chosen to maximize resistance to thermal shock, according to the criteria developed by Pfefferle (1980).

Knowledge of the physics of the new catalyst is essential for more realistic understanding and modeling of the heterogeneous rates. The steps to go from reactants to products in a catalytic process can be summarized as:

REACTANTS	gas-phase diffusion
	pore diffusion
	chemisorption on active sites
	chemical reaction(s)
PRODUCTS	pore diffusion
	products pore diffusion
	products gas phase diffusion

There is evidence that at the temperatures typical of catalytic combustion the surface of the catalyst is sintered to the point that the surface area available and geometric area practically coincide: for monolithic single-phase materials pore diffusion at high temperature may be also negligible; however, many

reactions are possible depending upon the chemisorbed species. For instance, in the CO/O_2 case, the possible states of the reactants are: (subscript a = adsorbed, g = gas phase)

1) CO_a and O_{2a}
2) O_{2a} and CO_g
3) CO_a and O_{2g}
4) CO_a and $O_g + O_g$
5) CO_g and O_aO_a
6) CO_a and O_a
7) CO_g and O_a

A Langmuir-Hinshelwood rate may be derived for each of these combinations. For instance, for 3) the rate of conversion of CO, r_c, is (Shishu, 1972)

$$r_c = \frac{K_s[A^2]K_{CO}K_{O_2}\left\{P_{CO}P_{O_2} - \frac{P_{CO_2}(P_{O_2})^{1/2}}{K_sK_{CO}K_{O_2}}\right\}}{(1 + K_{CO}P_{CO} + K_{O_2}P_{O_2})^2}$$

where K_{CO}, K_{O_2}, K_s are the equilibrium constants for adsorption of CO, O_2 and the forward rate of formation of active sites.

It is clear that only through a better knowledge of the surface can better rates be formulated. It is also extremely interesting to find which of the steps listed before is controlling. Given the single-phase structure of the proposed new catalyst, answers to the questions posed by the considerations above should be easier and far more reliable than for coated catalysts.

The actual forming of the flat plates and spacers made of the new catalyst was contracted with Trans-Tech, Inc., Gaithersburg, Md., a ceramic manufacturer. Perovskite powder to the specified stoichiometry was formulated and fabrication of the flat plates started approximately in December 1980. Several problems were

encountered in the process: the most important were an unexpected high sensitivity to the temperature and atmosphere composition of the furnace during the firing process, and severe warpage. The first problem made impossible for a long time the attainment of the desired density (and consequent mechanical properties). The second made very difficult or impossible the final grinding to the required geometrical dimensions. Solutions to these problems have currently evolved into a strategy of firing in forming gas at the elevated temperatures necessary for perovskite sintering (up to 1700 C), followed by reoxidation. Samples prepared in this manner are fully dense and appear to have good mechanical and thermal stability. The warpage has been attributed to a possible contamination by silica present in the Trans-Tech kilns during firing, and steps have been taken to control this. At the end of the contract for which this report is being written, test plates were being evaluated for platinum content and qualitative light-off behavior.

REFERENCES

H.V. Anderson, in Processing of Crystalline Ceramics, ed. H. Palmour et. al., Plenum, 1978.

Barr, R.F., and Watts, H., (1972), J. Chem. Eng. Data, vol. 17, no. 1, p. 45.

Biloen, P., Dautzenberg, F.M., and Sachtler, W.M.H., (1977), "Catalytic Dehydrogenation of Propane to Propene over Platinum and Platinum-Gold Alloys", J. Catalysis, vol. 50, p. 77.

Campbell, C.T., Ertl, G., Kuipers, H., and Segner, J., (1980), "A molecular beam study of the catalytic oxidation of CO on a Pt(111) surface", J. Chem. Phys., vol. 73, no. 11, p. 5862.

Engel, T., and Ertl, G., (1979), "Elementary Steps in the Catalytic Oxidation of Carbon Monoxide on Platinum Metals", in Advances in Catalysis, vol. 28, Academic Press, N.Y., p. 2.

Gardiner, W.C., and Olson, D.B., (1980), "Chemical Kinetics of High Temperature Combustion", in Annual Review of Physical Chemistry, Annual Reviews Inc., Palo Alto, p. 377.

Gosman, A.D., and Ideriah, F.J.K., (1976), "TEACH-T": A General Computer Program for Two-Dimensional, Turbulent, Recirculating Flow", Dept. of Mech. Engin., Imperial College, London, SW7.

Hautman, D.J., Dryer, F.L., Schug, K.P., and Glassman, I., (1981), "A Multiple-Step Overall Kinetics Mechanism for the Oxidation of Hydrocarbons", Comb. Sci. and Tech., vol. 25, p. 219.

Hautman, D.J. (1980), personal communication.

Howard, J.B., Williams, C.G., and Fine, D.H., (1973), "Kinetics of Carbon Monoxide Oxidation in Postflame Gases," XIV Symposium (International) on Combustion, The Combustion Institute, Pittsburgh, p. 975.

Kesselring, J.P., Krill, W.V., and Kendall, R.M., (1977), "Design Criteria for Stationary Source Catalytic Combustors," presented at the 2nd EPA Workshop on Catalytic Combustion, Raleigh, NC, June 21-22, 1977.

Lannus, A., (1970), Ph.D. Thesis, Drexel Institute of Technology, University Microfilm 70-24935, Ann Arbor, MI.

Meadowcraft, D.B., Brit. J. Appl. Phys. Sur. 2, 2, 1225 (1969).

Pfefferle, W.C., "Thermal Shock Resistant Catalytic Monoliths Using Foam Ceramics Technology," presented at 4th EPA Workshop on Catalytic Combustion, Cincinnati, OH, May 14-15, 1980.

Satterfield, C.N., (1980), Heterogeneous Catalysis in Practice, McGraw Hill Book Co., N.Y., p. 10.

Shishu, R.C., "Kinetics of CO Oxidation over Pt Catalysts," D.E. Thesis, Univ. of Detroit (1972).

Strozier, J.A., "Oxidation of CO on Pt by an AC Pulsing Technique - II: Experiment." Brookhaven National Laboratory Report BNL-25406.

Talley, L.D., Sanders, W.A., Bogan, D.J., and Lin, M.C. (1981), Internal Energy of Hydrozyl Radicals Desorbing from Polycrystalline Pt Surfaces," Chem. Phys. Letters, Vol. 78, No. 3, p. 500.

Talley, L.D., Tevault, D.E., and Lin, M.D., (1979), "Laser Diagnostics of Matrix-Isolated OH Radicals from Oxidation of H_2 and D_2 on Platinum," J. Chem. Phys., Vol. 72(5), p. 3314.

Voltz, S.E., Morgan, C.R., Liederman, D., and Jacob, S.M., (1973), "Kinetic Study of Carbon Monoxide and Propylene Oxidation on Platinum Catalysts," Ind. Eng. Chem. Prod. Res. Develop., Vol. 12, No. 4, p. 294.

Voorhoeve, R. et al., Ann. NY Acad. Sci., 272, 3 (1976).


FILMED
9-8